This document was prepared in conjunction with work accomplished under Contract No. DE-AC09-96SR18500 with the U. S. Department of Energy.

DISCLAIMER

WSRC-MS-2004-00663, Rev. 0
Distribution Category: Unlimited

Keywords: Glass durability, long term performance, surface layers

Retention: **Permanent**

GLASS DURABILITY MODELING: ACTIVATED COMPLEX THEORY (ACT) AND QUASI-CRYSTALLINE STRUCTURAL RATIOS (U)

Carol M. Jantzen and John M. Pareizs
Savannah River National Laboratory
Aiken, SC 29808

A paper for publication in the Journal of Nuclear Materials, Elsevier Publishing Co., Editors: L.K. Mansur (Chairman), Metals and Ceramics Division, Oak Ridge National Laboratory, P.O. Box 2008, Oak Ridge, TN 37831-6138, USA, (Email:mansurlk@ornl.gov) and/or L.O. Werme, Swedish Nuclear Fuel and Waste Management Co., Box 5864, S-10248 Stockholm, Sweden, (Email:skblw@skb.se).

GLASS DURABILITY MODELING: ACTIVATED COMPLEX THEORY (ACT) EXPRESSED BY QUASI-CRYSTALLINE STRUCTURAL RATIOS (U)

Carol M.Jantzen and John M. Pareizs
Savannah River National Laboratory
Aiken, SC 29808
carol.jantzen@srnl.gov

ABSTRACT

The most important requirement for high-level waste (HLW) glass acceptance for disposal in a geological repository is the chemical durability, expressed as a glass dissolution rate. During the early stages of glass dissolution in near static conditions that represent a repository disposal environment, a gel layer resembling a membrane forms on the glass surface through which ions exchange between the glass and the leachant. The hydrated gel layer exhibits acid/base properties which are manifested as the pH dependence of the thickness and nature of the gel layer. The gel layer has been found to age into either clay mineral assemblages or zeolite mineral assemblages. The formation of one phase preferentially over the other has been experimentally related to changes in the pH of the leachant and related to the relative amounts of Al^{+3} and Fe^{+3} in a glass. The formation of clay mineral assemblages on the leached glass surface layers (lower pH and Fe^{+3} rich glasses) causes the dissolution rate to slow to a long-term "steady state" rate. The formation of zeolite mineral assemblages (higher pH and Al^{+3} rich glasses) on leached glass surface layers causes the dissolution rate to increase and return to the initial high forward rate. The return to the forward dissolution rate is undesirable for long-term performance of glass in a disposal environment.

An investigation into the role of glass stoichiometry, in terms of the quasi-crystalline mineral species in a glass, has shown that the chemistry and structure in the parent glass appear to control the activated surface complexes that form in the leached layers, and these "mineral" complexes (some Fe^{+3} rich and some Al^{+3} rich) play a role in whether or not clays or zeolites are the dominant species formed on the leached glass surface. The chemistry and structure, in terms of Q distributions of the parent glass, are well represented by the atomic ratios of the glass forming components. Thus, glass dissolution modeling using simple atomic ratios is shown to represent the structural effects of the glass on the dissolution and the formation of activated complexes in the glass leached layer. This provides two different methods by which a linear glass durability model can be formulated. One based on the quasi-crystalline mineral species in a glass and one based on cation ratios in the glass: both are related to the activated complexes on the surface by the law of mass action. The former would allow a new Thermodynamic Hydration Energy MOdel (THERMO™) to be developed based on the hydration of the quasi-crystalline mineral species if all the pertinent thermodynamic data were available. Since the pertinent thermodynamic data is not available, the quasi-crystalline mineral species and the activated complexes can be related to cation ratios in the glass by the law of mass action. The cation ratio model can, thus, be used by waste form producers to formulate durable glasses based on fundamental structural and activated complex theories. Moreover, a glass durability model based on atomic ratios simplifies HLW glass process control in that the measured ratios of only a few waste components and glass formers can be used to predict complex HLW glass performance with a high degree of accuracy, e.g. an R^2~0.97.

1.0 INTRODUCTION

The most important requirement for high-level waste (HLW) glass acceptance for disposal in a geological repository is the chemical durability, expressed as a glass dissolution rate. Modeling of the chemical durability of glass, e.g. glass-solution interactions, has paralleled the modeling of mineral-solution durability in that the kinetic treatments have systematized the effects of pH, temperature, saturation state, ionic strength, and inhibition on the overall dissolution rate by developing models that treat each effect individually [1]. The kinetic effects of saturation state as a function of pH, temperature, and ionic strength have primarily been handled by the application of Transition State Theory (TST) and the free energy dependence of basic irreversible dissolution reactions [2, 3]. These TST and irreversible dissolution reactions are those currently being used to predict HLW waste glass dissolution in the Yucca Mountain geological repository in the United States [4].

The original kinetic treatment of mineral dissolution using the TST theory developed by Aagard and Helgeson [2] was followed by a rigorous demonstration that mineral dissolution was controlled by surface activated complex reactions, e.g. that the dissolution rate is controlled by reactions at the solid/aqueous solution interface, by activated complexes. This "surface reaction hypothesis" was the only mechanism that was deemed consistent with the TST theory and the irreversible thermodynamics used to derive the rate equations for the hydrolysis of minerals [5]. The TST kinetics and the irreversible thermodynamics on which it is based were deemed to be inconsistent with alternative durability hypotheses:

- "leached layer hypothesis" - control of exchangeable cations by diffusion through a nonstoichiometric leached residuum of the reactant solid while the leached aluminosilicate framework dismantles at a slower rate
- "armoring precipitate hypothesis" - diffusion through the interstices of a coherent surface precipitate (amorphous or crystalline) limits the rate of hydrolysis

1.1 Activated Complexes

Recently, the role of activated complexes has been integrated into the TST theory [6] and applied to glass dissolution as well as to mineral dissolution. This same approach was used to describe the inhibition of dissolution [7] for aluminosilicates. In this recent treatment of the role of activated complexes on chemical durability, the rate-limiting step is considered to be the destruction of the slowest breaking metal-oxygen bonds, e.g. those that are essential for maintaining the mineral or glass structure. Determination of which dissolution pathway is fastest, and thus rate controlling, requires the identification of any and all processes that could accelerate the destruction of the slowest breaking metal-oxygen bonds. For dissolution of feldspars (alkali aluminosilicates) the rate limiting step was found to be partial liberation of a metal by the removal of adjacent metals through previously equilibrated exchange reactions, e.g. an Al^{3+} is exchanged for $3H^{+}$ on the surface of the mineral or glass and this leads to the formation of three partially liberated Si atoms [6, 7] that then form a partially detached, slow-exchanging metal oxide precursor complex that is rate controlling. The activated complex has the same chemical formula as the precursor complex but the activated complex has more energy and represents some fraction of the precursor complex that is available for dissolution. The overall dissolution rate is, therefore, proportional to the quantity of these precursor complexes on the glass (or mineral) surface.

Moreover, an Activated Complex Theory (ACT) was proposed in 1988 by Wieland, Wehrili, and Stumm [8]. ACT was based on the concepts of Helgeson [5] and is consistent with the more recent approaches of Lasaga [9]. ACT was proposed to bridge the gap between thermodynamic information (surface coordination and lattice or site energy) and kinetic information. The ACT dissolution rate constant k is proportional to the free energy of conversion of the activated surface complex which is the rate determining step governing dissolution. This energy is, therefore, related to the activation energy of the rate-determining step in the dissolution. A simple reaction scheme can be written to illustrate the steps in the chemical dissolution of a glass (or a mineral) via activated surface complexes [6, 8]:

Equation 1 Glass ± aqueous species ↔ precursor complex ↔ activated complex → products

Only the last step in the dissolution process is considered irreversible (note directionality of last reaction in the sequence). For minerals that do not contain Al^{3+}, other metal/proton exchange reactions partially liberate the silica tetrahedral chains. In $MgSiO_3$ (enstatite) and Mg_2SiO_4 (forsterite) minerals the Mg/proton exchange is responsible for the partial liberation of the silica, and for $CaSiO_3$ (wollastonite) it is the Ca/proton exchange that is responsible for the partial liberation of the silica [6] precursor/activated complex.

The Al/proton exchange has also been shown to be the step that forms the precursor complex in basalt glass [10] dissolved in both acidic and basic solutions. The basalt glass dissolution is described as a rapid removal of univalent and divalent cations from the near surface followed by the Al^{3+} and $3H^{+}$ exchange. The breaking of the Al-O bonds does not destroy the glass framework but it partially liberates the silica tetrahedral chains as in the feldspar dissolution mechanism [6]. It is the detachment of this partially liberated silica that is the rate determining step, e.g. partially detached silica dissolves more readily than attached tetrahedral silica. The basalt glass dissolution is therefore proportional to the concentration of partially detached framework tetrahedral Si near the surface, which is linked through the law of mass action to the concentration of Al via the Al/proton exchange reaction. The concentration of Al in the glass is also linked to the aqueous aluminum activity in the leachate solution [6, 7] by the law of mass action [6, 7].

The Al/proton precursor/activated complex mechanism for basalt glass and crystalline albite ($NaAlSi_3O_8$) dissolution is in agreement with recent findings [11] of the French HLW R7T7 glass and a pure albite glass. The 2001 French study demonstrated that the TST rate equations only predict the glass alteration rate when a gel layer is missing or non-protective. These researchers hypothesized that the dissolution rate decreases by several orders of magnitude after an initial accelerated rate as the dissolution reaction progresses because a rate-limiting mechanism hampers mass transfer between the unreacted glass and the solution. It was hypothesized [12] that the glass dissolution rate was controlled by a multielement (Si-Al) activated complex in the leachate solution which was modeled as the ion activity product (IAP), $a_{Si}^{0.88} \times a_{Al}^{0.12}$, where the ratio of Si:Al in the IAP was proportional to the Si:Al ratio in the glass (normalized to 1). In these experiments the SiO_2 activity in solution was kept constant and only the $Al(OH)_4^-$ activity in solution was varied. Small changes in the activity of the $Al(OH)_4^-$ aqueous species had a major impact on the glass dissolution kinetics. Additional studies confirmed that the glass dissolution was controlled by both glass composition and the chemistry of the fluid contacting the glass [13].

The relationship between the stoichiometry of the precursor and activated complex and the parent glass or mineral species is further substantiated by the original work of Helgeson et al. [5] who carefully analyzed various experimental data to determine the mineral dissolution rate of crystalline albite as a function of pH. They related these findings to experimental work by Lagache [14] who had determined that $(H_3O)AlSi_3O_8$ served as a reactant and formed an activated complex on the mineral surface which controlled the dissolution rate of the feldspar minerals, e.g. $(Na,K)AlSi_3O_8$ a solid solution of albite and orthoclase. While the exact activated complex was determined to be different in different pH ranges, the stoichometry of the activated complex in terms of the Al:Si ratio was always the same as the Al:Si ratio of the parent mineral dissolved:

- at pH <2.9 $((H_3O)AlSi_3O_8(H_3O))^+$
- at pH 2.9 -8.0 $(H_3O)AlSi_3O_8(H_2O)n$
- at pH >8.0 $(Na,K)Al(OH)_nSi_3O_8^{n-}$

1.2 Activated Complexes and the Relation to the Quasi-Crystalline Structure of Glass

The relation between Al and Si in the Activated Complex Theory (ACT) implies that the stoichiometry of the precursor (and activated) complexes are related to the stoichiometric structure (Q distribution[‡]) of the parent glass (or mineral) and this has been shown by recent research on glasses made from a single mineral compositions (see Figure 1). Glasses and feldspars with more Al^{3+} compared to Si^{4+} have been found to dissolve at higher rates [7,15] in proportion to the Al:Si ratios. Additional research performed on simple sodium aluminosilicate glasses of various mineral compositions also supports the controlling role of an activated aluminosilicate reaction on glass dissolution. The altered layers of simple glasses with a $NaAlSiO_4$ (nepheline) composition, a $NaAlSi_2O_6$ (jadeite) composition, and a $NaAlSi_3O_8$ (albite) composition were examined by Nuclear Magnetic Resonance (NMR) techniques. These studies showed that Al^{VI} is present in the leached layer versus Al^{IV} in the glass and that the fraction of Al^{VI} in the altered layer increased with increasing duration of dissolution. In addition, the dissolution rate was proportional to the ratio of $Al^{VI}/(Al^{VI} + Al^{IV})$ and the Al/Si of the parent glass [15,16, 17], e.g. durability decreased going from albite to jadeite to nepheline glass.

The correlation with the stoichiometry of the parent glass is important as the Al-O-Si linkages in the glass are known to hydrolyze more rapidly than the Si-O-Si bonds [6, 7, 10, 18], e.g. hydrolysis of Al-O-Si bonds becomes more energetically favorable as the number of Al atoms per Si tetrahedron increases [15]. Based on depth-profiling of leached layers using X-Ray Photoelectron Spectroscopy (XPS), Hellmann and others [19] proposed an activated complex where H_3O reacts with the bridging oxygen (O_{br}) site in a $\equiv Al\text{-}O_{br}\text{-}Si\equiv$ linkage which then decomposes to $\equiv Al - OH_2^+$ and $\equiv Si - OH$. These authors also discussed their experimental findings of a surface activated complex in regards to TST theory and other activated alumina complexes suggested by Helgeson, et al. [5].

---

‡ The polymerization or extent of medium-range order of a melt can thus be expressed by calculating or measuring a Q distribution, e.g. the number of Q^4, Q^3, Q^2, Q^1, and Q^0 species in a simple two or three component melts. The Q^n is the number of bridging oxygen (BO or O_{br}) atoms linked to a given Si atom (where n=0, 1, 2, 3, or 4). The number of Q^4 units in a melt, e.g. silica tetrahedra that have not reacted with a metal cation to form a non-bridging oxygen (NBO or O_{nbr}), can be correlated to the thermodynamic activity of SiO_2 in the melt.

1.3 Impact of Al^{+3} and Fe^{+3} on Nuclear Waste Glass Durability Modeling

The ACT approach indicates that if the quasi-crystalline Q distributions in a glass could be measured or otherwise estimated that these would be proportional to the overall glass dissolution rate. The ACT approach to chemical durability also indicates that the role of multi-element species that participate in the glass network, e.g. Al^{3+} and Fe^{3+}, have been underestimated during nuclear waste glass dissolution modeling.

Additional reasons for investigating the role of Al^{3+} and Fe^{3+} being liberated from a HLW waste glass at a constant stoichiometric ratio, a ratio related to that of the parent glass, comes from the observations of Van Iseghem and Grambow [20] who demonstrated that an Al^{3+} rich zeolite (analcime) forms on certain glasses during their dissolution. The formation of analcime in these experiments carried out at 90°C at SA/V conditions of 10, 100, and 7800 m^{-1} accelerated the glass corrosion by consuming H_4SiO_4 from the leachate solution but did not accelerate the glass corrosion back to the original forward rate, e.g. "the formation rate of analcime is too small to bring the glass dissolution rate back to the forward rate" [20]. The two glasses studied, SM58 and SAN60, contained 1.2 wt% Al_2O_3 and 1.2 wt% Fe_2O_3 (SM58) and 18.1 wt% Al_2O_3 and 0.3 wt% Fe_2O_3 (SAN60). The SAN60 glass with the highest concentrations of Al_2O_3 and the lowest amount of Fe_2O_3 was the glass that formed the analcime reaction product. These authors also demonstrated that a change in solution pH accompanied the return to the forward rate when analcime formed. Likewise, Inagaki [21] demonstrated that solution pH and solution concentrations of Na and K were also involved in the formation of analcime versus Na-bedellite (a smectite clay). Other zeolites and smectite clays that are rich in Fe^{3+} compared to Al^{3+} do not appear to accelerate glass corrosion [20, 22].

The return to a forward dissolution rate is undesirable for the long term durability of HLW glass and raises the question: Can HLW glasses be formulated to avoid analcime formation and thus avoid a return to the initial high forward rate of dissolution? Recent modeling efforts by Strachan and Croak [23] demonstrated that HLW glasses were predicted to be very stable with respect to analcime formation as long as the ratios of Si/(Si+Al) in cation percent were ≥ 0.7 and the cation ratios Na/(Na+Li), Na/(Na+Ca), and Na/(Na+B) were between 0.2-1.0 percent. These ratios were calculated from equilibrium geochemical models using only the glass composition. The ratios were shown to be non-linear functions of the "degree of reaction progress," a parameter in the TST kinetic equations used to describe waste glass chemical durability: a glass on the reaction progress plateau was deemed to be very stable with respect to analcime formation for the cation ratios given above.

The current investigation demonstrates that the parent glass can be represented as a mixture of quasi-crystalline mineral species. The residual gel can be represented as the reaction products predicted to be in equilibrium with the aqueous chemistry of experimental leachates, and that the two are related, e.g. proportional due to the law of mass action as shown by Oelkers et al. [6, 7]. This allows a chemical relationship to be derived between the glass composition and the composition of the gel layer derived from the leachate concentrations (Figure 1). This approach demonstrates that the structure in the parent glass, especially the role of Al^{3+} and Fe^{3+}, and the role of $Al(OH)_4^-$ and $Fe(OH)_4^-$ in the solution, control the formation of the activated surface complexes that in turn age into either zeolite or clay mineral assemblages.

The structural distributions of the parent glass are shown to be represented by the atomic ratios of the glass forming components. This provides a glass durability model that can be used by waste

form producers to formulate durable glasses, including high alkali glasses, while describing basic glass durability mechanisms since mechanistically based models are preferred by the geological repository [24]. In addition, a glass durability model based on atomic ratios simplifies HLW glass process control in that the measured ratios of only a few waste components and glass formers can be used to reliably predict HLW performance.

2.0 BACKGROUND

2.1 Stages of Glass Dissolution

Typically during the glass dissolution process in near static conditions representing a repository disposal environment, there is a short period of alkali proton-hydronium ion-exchange followed by matrix dissolution and/or solution precipitation/condensation reactions [25,26]. This initial rapid rate of ion-exchange is commonly known as the forward rate (Stage I) of glass dissolution (Figure 2).

The forward glass dissolution rate is modified by a rate-limiting mechanism hypothesized to be related to the activated complexes being formed that become components of the gel layer or activated complexes in solution. Thus the gel layer is composed of hydrated silica, alumina, and ferria and other large, highly charged cations (high Z/r ratio cations where Z is the atomic charge and r is the atomic radius). The glass reaction zone is defined as the leached layer solution interface where equilibrium is considered to be between the glass surface sites and the ions in solution [27]. The top of the gel reaction zone represents the leached layer glass interface where a counter-ion exchange occurs [27] that can form secondary precipitates, e.g. metal hydroxo and/or metal silicate complexes that have reached saturation in the leachate often precipitate on the surface of the gel layer [25, 26, 28, 29, 30, 31]. The gel layer may, under certain conditions, act as either or both a selective membrane [28, 32] or as a protective/passivating layer [25, 26, 30, 31, 33, 34, 35, 36, 37]. The slowing of the glass dissolution to a steady state rate by any combination of the above mechanisms is referred to as Stage II or steady state dissolution (Figure 2).

Glass dissolution has been accelerated in static laboratory scale tests by increasing the glass surface area (SA) exposed to a given volume of leachant (V), e.g. performing crushed glass tests, and/or by extending the test duration (t in days) to long times, and/or by increasing the test temperature (T). Testing can be accelerated in monolithic glass laboratory scale tests by increasing the test temperature, increasing the test duration, and/or by using steam. Based on the early experiments on window glass [38] in saturated steam (150-200°C), the higher the temperature and the more saturated the steam, the greater the penetration of the H_2O and OH^- into the glass and the more rapidly an altered gel layer is formed. Much progress has been made in the accelerated durability testing of nuclear waste glasses using the Vapor Hydration Test (VHT) [39]. In VHT testing a nominal temperature of 200°C is used and exposure of the glass to steam causes a high effective SA/V [39,40].

Studies have shown [41] that glass durability test acceleration using the (SA/V)•time parameter is only valid up to values of ~20,000 m^{-1}, at which point there is a possible change in mechanism for some glasses. There is evidence from poorly durable glasses such as the Defense Waste Processing Facility (DWPF) Environmental Assessment (EA) glass that at 20,000 m-1 that all of the glass has been completely reacted [42]. This change in mechanism causes the long-term dissolution rate to reaccelerate at the initial forward dissolution rate for some glasses. This

unexpected, and poorly understood, return to the forward dissolution rate (Stage III) has been shown to be related to the formation of the Al^{3+}-rich zeolite, analcime, and/or other calcium silicate phases [20] at (SA/V)•time values between 20,000 m^{-1} and 100,000 m^{-1}. Use of the (SA/V)•time acceleration parameter, has widely been used to relate the response of a variety of laboratory glass durability tests to each other. For example

- short- and long-term monolith tests (ASTM C-1220, MCC-1) have been related to short- and long-term crushed glass tests (ASTM C-1285, PCT, MCC-3) [28, 43, 44, 45]
- short- and long-term monolith tests have been related to long-term burial tests [46, 47]
- the response of long term crushed glass tests (ASTM C-1285, PCT) have been related to shorter term, higher temperature, vapor hydration test (VHT) responses, e.g. the Defense Waste Processing Facility (DWPF) Environmental Assessment (EA) glass reaches Stage III durability within 56 days at 20,000 m^{-1} or >313 days at 2000 m^{-1} when tested by PCT at 90°C [45] or within 6 days when tested by VHT at 200°C [45]
- the forward rate of a short term monolith test (ASTM C-1220, MCC-1) has been shown to be equivalent to the forward rate of the single pass flow though (SPFT) test [4, 45]
- the forward rate of the short term crushed glass test (ASTM C-1285, PCT) has been shown to be an upper bound for Stage II and Stage III durability behavior [4, 45]

However, research has shown [48] that different pH values are achieved during static testing at different SA/V and that this may affect the reaction rate and the phases that form and must be accounted for when comparing the results of tests at equivalent SA/V•t. In addition, it must also be demonstrated that the glass alteration is equivalent and that the corrosion mechanism is the same at different SA/V•t [48].

2.2 Stage III Dissolution: Aging of Leached Aluminosilicate Layers

Experimental aging of the hydrated gel layers formed during Stage III glass dissolution has shown that the gel layer components age in situ into either clay mineral assemblages or zeolite mineral assemblages [49, 50, 51, 52, 53]. In order to understand the aging of a leached glass gel layer into either clay or zeolite mineral assemblages, it is important to recognize that the hydrated gel layer exhibits acid/base properties which are manifested as the pH dependence of the thickness and nature of the gel layer [54]. Thus, if the solution pH changes while the gel ages a clay mineral species may convert into a zeolite mineral species in response to an increase in pH. However, in a repository where pH control is dominated by other factors such as groundwater chemistry, such pH responses should not occur.

The in-situ aging of an aluminosilicate rich reaction layers in HLW glasses mimics the aging of aluminosilicate gels, both artificially produced gels and those found in nature. Aluminosilicate gels that were co-precipitated under controlled laboratory conditions were aged into a variety of natural clays (smectities, beidellites, saponites, sauconites and montmorillonites) [55, 56, 57]. Aluminosilicate gels found in natural geothermal systems in an alkaline environment were harvested and then aged in the laboratory to the zeolite analcime [58]. The alteration of aluminosilicate gels (artificial or natural) to clay or zeolites is pH dependent, with clay formation

favoring less basic aging environments than zeolites [59]. Aging of leached gel layers in natural environments, e.g. weathering of altered rhyolitic (acidic) volcanic glass, has been shown to alter in situ to both zeolites (clinoptilolite) and clays (smectitie, montmorillonite), and sometimes opal (hydrous silica) [58, 60, 61].

Sequential aging of nuclear waste glass gel layers under controlled laboratory conditions produced montmorillonite clay [62]. In addition, the in situ formation of smectite clays has been determined to be dependent on the iron content of the dissolving glass [63]. The similarity of gel layer formation and dissolution mechanism of borosilicate waste glasses containing iron and natural basalt glasses containing iron has recently been documented by Morgenstein [64] and previously by Ewing [65], Malow [66], Allen [67], and Jantzen [68]. In particular, the work of Allen [67] indicated that the alteration layer on basalt glass is formed of cryptocrystalline iron rich clays grouped under the term "palagonite." Likewise, the geochemical modeling (EQ3/EQ6) performed by Bourcier [69] on an iron rich waste glass gel layer composition predicted the formation of notronite ($Fe_2Si_2O_7 \bullet 2H_2O$) the iron analogue of the Al-rich clay mineral kaolinite ($Al_2Si_2O_7 \bullet 2H_2O$). Additional comparisons of the aging sequences of basaltic glasses and nuclear waste glasses tested by VHT have indicated the following aging sequences (paragenic trends) [52, 53]:

Equation 2 unaltered glass $\rightarrow$ smectite clays $\rightarrow$ (alkalic silicic zeolites)* $\rightarrow$ analcime

---------- increasing solution pH ----------$\rightarrow$

which upon further aging, including dehydration, may form anhydrous feldspars (K-rich and Na-rich species such as albite). Often the alkalic silicic zeolite phases do not form and smectite clays are found to be in contact with analcime. This paragenetic sequence shown in Equation 2 occurs as the solution becomes more basic and more saturated with silica and alumina during static durability testing.

The waste glass gel layers are zoned (5-7 zones) and the paragenic sequences of the layers follow the sequence shown in Equation 2 [52, 53]. The smectite clays are always in contact with the unaltered glass while analcime is further removed [52, 53, 70]. Glasses rich in K are found to form $KAlSi_3O_8$ (orthoclase) in the surface layer and glasses rich in Ca form $Ca_4(Si_6O_{16})(OH)_2 \bullet 3H_2O$ (gyrolite), $Ca_5(PO_4)_3OH$ (Hydroxy apatite), and/or $Ca_5(OH)_2Si_6O_{16} \bullet 4H_2O$ (tobermorite) [48, 70]. For glasses containing U, a uranium silicate often forms such as $K_2(UO_2)_2(Si_2O_5)_3 \bullet 4H_2O$ (weeksite) [70] or $KNa_3(UO_2)_2(Si_4O_{10})_2(H_2O)_4$ [71].

The paragenic sequences found in the aged leached gel layers are the same as those found in natural deposition basins as alkalinity of the water in the basin increases [52, 53]. This indicates that the aging sequences observed during HLW glass leached layer aging may, indeed, be a function of changing alkalinity caused by the closed and static nature of the test which prevents the alkali and alkaline earth species released from the glass from migrating away from the aluminosilicate rich gel produced during dissolution. It also suggests that the role of pH and the role of Al^{3+} and Fe^{3+} in the solution are key parameters that drive the species that form during Stage III dissolution and whether or not a given glass will exhibit Stage III dissolution behavior.

* these phases were sometimes but not always observed, e.g. Na-chabazite ($Na_2Al_2Si_4O_{12}) \bullet 6H_2O$ or chabazite ($CaAl_2Si_4O_{12}) \bullet 6H_2O$

3.0 EXPERIMENAL/MODELING

A database of over 600 glasses that had been durability tested using the ASTM C-1285 (PCT Methods A and B) test in deionized water was compiled. The leachate concentrations for each glass represent the mean of three tests performed at 90°C. The ASTM C-1285 Test Method A is used in the United States for the routine testing of HLW glass product consistency under prescribed conditions, e.g. closed system (stainless steel vessels), 90°C and 7 day duration. Use of a forward rate deconvoluted from the results of the ASTM C-1285 Test Method A was recently shown to be an upper bound for Stage II and Stage III durability behavior [4, 45]. ASTM C-1285 Test Method B can be performed under the same test conditions in Teflon® vessels or at varying temperatures (T), test durations (t) or surface area to leachate volume (SA/V) ratios. Leachate test results can be reported in ppm, grams of waste form dissolved per liter of leachate (g/L), grams of waste form dissolved per square meter of surface area per day ($g/m^2 \bullet day$), or grams of waste form dissolved per square meter of surface area (g/m^2). In this modeling study the mean ppm of the triplicate leachates are converted from ppm to millimoles/L of solution for each leachate species of interest. This is done because the leachate input to the geochemical software used requires millimoles/L. In addition, the leachate solution concentrations are modeled in millimoles/L instead of in normalized mass loss as done in previous studies [78,79] because normalized mass loss has a measured glass composition term in the denominator that can add error to the dependent modeling term when regressed against the independent glass composition modeling term.

The short term (7-day PCT-A) durability database includes data for borosilicate waste glasses from six different statistically designed studies (Table 1). These designed studies include the Matrix Glass (MG) study in the Na_2O-B_2O_3-SiO_2-Al_2O_3-Fe_2O_3-CaO system [72], studies (BK and C) of defense waste glass compositions [73,74], studies (R and REE) concentrating on high Fe_2O_3 containing Purex waste glasses [75,76], and a recent study (RX) [77] assessing the role of REDuction/OXidation (REDOX) on glass durability. The MG glasses comprised a subset of 33 glasses (designated MG glasses for matrix glass) that had been statistically designed in the 6-component oxide system Na_2O-B_2O_3-SiO_2-Al_2O_3-Fe_2O_3-CaO system to go well beyond the range of HLW borosilicate glasses being produced at the Savannah River Site (SRS). An extreme vertices statistical design was employed to design the MG glass composition region. Glasses MG-1 through MG-20 comprises the extreme vertice glasses in mol oxide percent. Glasses MG-21 through MG-33 represents the centroid glasses where glasses MG-21 through MG-32 are the face centroids of the composition region and MG-33 is the overall centroid of the region. The glasses were melted at temperatures ranging from 1150-1500°C.

In addition, the data originally used in the development of the THERMO™ glass durability model [78,79], glasses from a round robin conducted at SRNL on the Waste Compliance Plan (WCP) glasses that span the entire range of the glasses anticipated for processing at the SRS [80,81], and glasses from a round robin conducted on the Environmental Assessment glass [82,83] were used during modeling (Table 1). The THERMO™ glass data set included glasses made in crucibles and glasses made in large scale pilot scale melters. In addition, data from HLW glasses taken from full scale canisters poured during the startup of the Defense Waste Processing Facility (DWPF) at the SRS during Qualification Runs (sections and grab samples), and radioactive glasses from the SRS M-Area facility [84] were included in the modeling database (Table 1). While the DWPF glasses are enriched in Fe_2O_3 compared to Al_2O_3, the M-Area glasses are enriched in Al_2O_3 and deficient in Fe_2O_3. The ranges of glass compositions studied are given in

Table 2 and compared to the compositions of the glasses studied by Van Isenghem and Grambow [20].

The glasses modeled from the THERMO™ study including the DWPF startup frit, the EA glass and the WCP glasses were analyzed from 4-10 times each by Corning Engineering Laboratory Services (CELS). Each was determined to be amorphous by X-ray Diffraction (XRD) analysis (Table 1). The DWPF full scale canister glasses and grab samples from the DWPF Qualification Runs, the pilot scale glasses (HG glasses and IDMS glasses), the M-Area glasses, the BK study and C study glasses were all analyzed by the SRNL Analytic Development Section (ADS) in duplicate (Table 1). The glasses from DWPF Qualification runs, the C study glasses, the M-Area glasses and the Startup frit and EA glasses were all determined to be amorphous by XRD analysis. The homogeneity of the BK glasses is unknown as XRD analyses were not performed (Table 1). The RX study glasses were analyzed by the SRNL Mobile Laboratory (ML) and appeared homogenous visually (Table 1). Additional Scanning Electron Microscopy (SEM) and Transmission Electron Microscopy (TEM) were performed on some glasses to determine their homogeneity as indicated in Table 1.

The THERMO™ glasses, the M-Area glasses, and the MG study glasses were tested in Teflon® vessels, e.g. open system tests. The WCP and EA glasses were tested in both Teflon® vessels and stainless steel vessels. The remaining studies were all performed in stainless steel vessels using the PCT-A, e.g. closed system tests (Table 1).

The glass modeling database was constrained in the following manner. If glasses had crystallized during fabrication they were not used for modeling since they were not truly amorphous and the effects of grain boundary dissolution may have impacted the modeling. If the REDOX of a glass was >0.33 $Fe^{+2}/\Sigma Fe$, which is beyond the operational range of waste glass melters due to crystallization of metals and metal sulfides, the glass was not used for modeling. If the measured glass oxide chemistry did not sum to 100±5 wt% the composition was considered to be too inaccurate for modeling. Lastly, if a glass had <3.5 wt% Al_2O_3 or >15 wt% B_2O_3 the glass was potentially phase separated and could give an anomalous durability response [85,86]. These low Al_2O_3 and high B_2O_3 glasses were not used for modeling. The <3.5 wt% Al_2O_3 constraint removed all of the glasses from the Purex waste (R and REE) studies from consideration. If a glass had been determined to be phase separated by SEM or TEM analysis it was not used in modeling.

The remaining glass database consisted of 329 glasses that had been tested using a 7-day ASTM C1285 test regardless of vessel type. The data modeled in this study span the range of the Strachan and Croak [23] glasses in the Na_2O-Li_2O-CaO-SiO_2-B_2O_3-Al_2O_3 system (Table 3) but also include the role of Fe_2O_3. The additional ranges of Si/Si+Fe and Fe/Fe+(Ca+Mg) for the glasses used for modeling in this study are shown in Table 3. The MG and the BK statistical studies span the largest composition range of the statistically designed databases used for modeling.

Twenty nine of the statistically designed MG glasses [72] were tested at long test durations (24 weeks) in Teflon® vessels (Product Consistency Test Method B, PCT-B), e.g. up to SA/V•t values of 336,000 day/m (at a constant SA/V of 2000 m^{-1}). Six glasses were tested for the same time duration in J-13 Yucca Mountain geological repository ground water. Both the MG glasses and the THERMO™ crucible study glasses were also leached for 2 weeks and 4 weeks up to

SA/V•t values of 56,000 day/m (at a constant SA/V of 2000 m^{-1}) at 90°C (Table 1). Therefore, two databases were constructed, one for short duration (7 day) tests which was used for both leachate modeling and geochemical calculations and one for long duration (2-24 week) testing which was only used for geochemical calculations. Both databases included leachate concentrations for Na, Li, K, Ca, B, Si, Al, and Fe.

The short-term and long-term leachate solutions were modeled with Geochemist's Workbench (GWB) to determine the most saturated phases in the solution and thus the potential steady state phases in equilibrium with the leached gel layer. The GWB modeling and assumptions are described in Appendix I. All thermodynamic calculations presented in this study were performed using GWB Version 4.0 and the latest revision of the thermodynamic data in the Lawrence Livermore National Laboratory (LLNL) EQ3/EQ6 database [87].

In order to relate the phase predictions from GWB to the glass composition and glass durability, results from time sequence tests of the MG glasses that were performed at 1 week, 2 weeks, 4 weeks, and 24 weeks corresponding to SA/V•t values of 14,000 day m^{-1}, 28,000 day m^{-1}, 56,000 day m^{-1}, and 336,000 day m^{-1} were preferentially used. All of the long term data were used in geochemical modeling since the effects of back reactions in static tests can influence the congruent relationships between the release of Na, Li, B, and Si. The short term data was constrained to leachate data that demonstrated that the normalized release of B (g/L) was congruent with the release of Li (g/L), Na (g/L), and Si (g/L).

4.0 MODELING THE QUASI-CRYSTALLINE SPECIES IN HLW GLASSES

The use of Infrared (IR) and Raman spectroscopy has demonstrated that glasses are not totally random structures and that there is "speciation" within the glass network due to polymerization [88]. For alkali silicate glasses, Raman band intensities defined framework units, sheet-like units, chain-like units, and monomers. Therefore, a computer model, NORM-CALC™, was developed to calculate the most likely polymerized quasi-crystalline[f] mineral components of a glass. This approach is based on the principle of normative mineral calculations used in geochemistry [89], e.g. the so called Cross-Iddings-Pirsson-Washington or C.I.P.W. calculation, for calculating the mineral species that would form from a natural glass if it were allowed to slowly crystallize and reach equilibrium. The C.I.P.W. normative calculations are based on the known principles of mineral crystallization from molten magmas, e.g. natural glasses enriched in both ferria and alumina. Use of C.I.P.W. normative mineral components in fiberglass and nuclear waste glasses was recently described by Condrat [90,91] as a method to relate glass composition to glass durability. In addition, Condrat has used the C.I.P.W. normative calculations to predict melt rate,

---

[f] Glasses and natural silicate melts, possess no long-range structural periodicity or symmetry like crystalline materials. Glasses do possess short-range order (radius of influence ~1.6-3Å) around a central atom, e.g. polyhedra such as tetrahedral and octahedral structural units [G.E. Brown, Jr., F. Farges, and G. Calas, **"X-Ray Scattering and X-Ray Spectroscopy Studies of Silicate Melts,"** Structure, Dynamics and Properties of Silicate Melts, J.F. Stebbins, P.F. McMillan, and D.B. Dingwell (Eds.), Reviews in Mineralogy, V.32, 317-410, 1995]. Glasses and melts also possess medium-range order which encompasses second- and third-neighbor environments around a central atom (radius of influence ~3-6 Å). The more highly ordered regions, referred to as clusters or quasi-crystals, often have atomic arrangements that approach those of crystalline mineral species [C.W. Burnham, **"The nature of multi-component aluminosilicate melts,"** Phys. Chem. of the Earth, v. 13 & 14, 191-227, 1981].

the theoretical heat demand of the batch-to-melt conversion, and later confirmed this normative mineral model with calorimetric measurements [92].

The quasi-crystalline species used in this study were chosen to be consistent with known measurements and/or molecular dynamic (MD) simulations in simple three and four component glass systems. The NORM-CALC™ computer program was written in JMP software to calculate the quasi-crystalline groupings in the >300 waste glasses modeled. As in the C.I.P.W. normative calculations, the most polymerized alkali aluminosilicates form first, e.g. $KAlSi_3O_8$ (orthoclase) and $NaAlSi_3O_8$ (albite). After speciation of the $KAlSi_3O_8$ any excess Al (in cation %) was speciated first as $NaAlSi_3O_8$. If there was not enough Al in the glass to form an alkali silicate with a cation% Al:Si ratio of 1:3, then $NaAlSi_2O_6$ (jadeite) was allowed to form preferentially. If there was not enough Al in the glass to form an alkali silicate with an Al:Si ratio of 1:2, then $NaAlSiO_4$ (nepheline) was allowed to form preferentially. Any excess K remaining after the formation of $KAlSi_3O_8$ was allowed to form a K-rich nepheline solid solution $(Na,K)AlSiO_4$. The speciation of the alkali aluminosilicates is in agreement with MD studies of Stein and Spera [93] in the $NaAlSiO_4$-SiO_2 system in which albite, jadeite, and nepheline glasses had similar structures to their crystalline mineral counterparts. The assumptions are also consistent with the NMR analyses of Tsomaia et al. on these mineral glasses [16,17] and the X-ray Photoelectron Spectroscopy (XPS) data of Smets and Lommen [94] that showed that no non-bridging oxygen atoms exist in an alkali aluminosilicate glass when the ratio of Al:Na is $\geq$0.75 which it is for albite, jadeite, and nepheline type glasses. The Al^{3+} is primarily tetrahedral and fully polymerized as Q^4 species [95]. Indeed, MD simulations have shown that when Al^{3+} enters a Na_2O-SiO_2 glass it moves Na^+ from alkali-rich channels into Al-silicate cages [96, 97].

The Na (cation %) and Si (cation %) not consumed in the formation of the alkali aluminosilicates are speciated with boron as $NaBSi_3O_8$ (reedmergnerite) in NORM-CALC™. Reedmergnerite has the albite structure [98] where B^{3+} replaces Al^{3+}. Glasses containing reedmergnerite structures have been shown to leach similarly to glasses containing albite structural units [99]. If the glass composition is either Na or Si deficient and cannot form the reedmergnerite stoichiometry of 1:1 Na:B or 1:3 B:Si, then $Na_2B_4O_7$ (sodium diborate) is formed preferentially to reedmergnerite. This is similar to the manner in which reedmergnerite groups have been calculated by others [72, 99, 100]. The reedmergnerite component represents the tetrahedral Q^4 boron while the diborate represents the trigonal Q^3 borate creating one non-bridging oxygen bond [100]. This is in agreement with the XPS studies of Smets and Lommen [94], the NMR studies of Geisinger et al. [95], and the NMR studies of Darab et al. [101] on Hanford Low Activity Waste (LAW) glasses in the Na_2O-Al_2O_3-B_2O_3-SiO_2 system. It is also consistent with the work of Smets and Krol [102], and Konijnendijk [103] who demonstrated that for sodium silicate glasses with low B_2O_3 content that B_2O_3 enters the glass network as BO_4^- tetrahedra and at higher concentrations these tetrahedra are converted into planar BO_3^- groups. Tetrahedral BO_4^- contribute no NBO while planar BO_3^- groups contribute one non-bridging oxygen atom [104].

Next NORM-CALC™ speciates excess cation% B as $Li_2B_4O_7$ (lithium metaborate). Excess cation% B over cation% Li is speciated as $Na_2B_4O_7$ (sodium metaborate). This sequence was chosen based on the assumption that the smaller cations with high polarizing energies such as Li will preferentially complex with the boron over the larger Na cations. Any excess cation % B over cation% Li and Na is speciated as B_2O_3 which is most likely present as boroxol groups or rings as in vitreous B_2O_3 [103].

Next the Fe^{+3} is speciated between two pyroxene chain structured minerals commonly found as devitrification products in high Fe_2O_3 containing waste glasses, augite ($(Ca,Mg)(Al,Fe^{+3})_2SiO_6$) and acmite ($NaFeSi_2O_6$) [105, 106, 107, 108]. Acmite and nickel iron spinel [105, 106] are the species that most readily crystallize in alkali HLW glasses containing 10-14 wt% Fe_2O_3. It should be noted that all of the iron in the glasses modeled is considered to be Fe^{3+} in the NORM-CALC™ glass calculation since the effects of Fe^{2+} on HLW glass durability have recently been shown [77] to be minimal in the range of REDOX equilibria normally achieved in HLW glass melters.

Since experimentation on Hanford LAW glasses has shown that divalent species such as Ca^{2+} do little to charge compensate tetrahedral Al and B, it is more likely that divalent species such as Ca^{2+} and Mg^{2+} complex with Fe to form pyroxene chain-like structures in the glass. This is consistent with the treatment in the C.I.P.W. normative calculations. Therefore, NORM-CALC™ uses a combination of the Ca, Mg, Fe, and residual Al leftover from speciation of the alkali aluminosilicates to determine the molar amount of augite that can potentially form. First the Ca (cation %) and Mg (cation %) are speciated with any remaining Al left after the alkali aluminosilicates have been formed and with any Fe (cation %) in the glass. For glasses that have insufficient Al or Fe to form augite, the Ca and Mg are calculated as another pyroxene phase, diopside, $(Ca,Mg)Si_2O_6$.

The residual Na and Si leftover after the formation of the alkali aluminates and reedmergnerite are speciated with the Fe^{+3} remaining after the formation of ferric augite and aluminous augite as $NaFeSi_2O_6$ (acmite) which is isostructural with $NaAlSi_2O_6$ (jadeite). In the absence of a Ni containing quasi-crystalline phase, excess Fe^{3+} over the amount of Na and Si available is speciated as Fe_2O_3. The calculations of the molar amounts of the pyroxenes known as augite, acmite, and diopside are consistent with the way Al and Fe phases are calculated for natural magmas [89], e.g. the C.I.P.W. normative calculations, and consistent with the devitrified product phases found in HLW glasses [105, 106, 107, 108].

For glasses with excess residual Al compared to Ca, Mg, and Fe, NORM-CALC™ speciates any excess Al (cation %) as Al_2O_3. Attempts to speciate the excess Al as the Li pyroxene known as spodumene ($LiAlSi_2O_6$), a phase also observed upon devitrification of high Li containing glasses [73, 107, 108], produced only one glass with this phase, e.g. one glass that had sufficient Li, Al, and Si to form this phase. Since one glass was statistically insignificant in terms of providing a technical basis for the species spodumene, this term was replaced with speciation of excess alumina as ™Al_2O_3.

Any excess Na and Si over the amount of Fe^{3+} available is speciated as Na_2SiO_3 in NORM-CALC™. Any excess Na over the amount of Si available is speciated as Na_2O. Likewise any residual Li after speciation as Li borate is speciated as Li_2SiO_3 which is also a phase commonly found to crystallize in HLW glasses [105, 106] and lastly as Li_2O. Any residual Si is speciated as SiO_2.

The role of minor species such as NiO, MnO, TiO_2, and ZrO_2 is not considered in the current model. For brevity, Table 4 gives selected glass compositions in terms of the mole% of the calculated quasi-crystalline mineral species, e.g. the output from NORM-CALC™,[f] and indicates the maximum mole% of each quasi-crystalline species calculated in the entire database.

[f] When the NORM-CALC™ species are converted to wt% the sum of the normative species for >90% of the glasses is within 95-100 wt% indicating mass balance has been achieved based on the measured

When pertinent thermodynamic data becomes available for species such as reedmergnerite, the quasi-crystalline species can be used to calculate a hydration free energy based on these species. In the meantime, a phenomenological approach can be used to target glasses that are composed of durable rather than non-durable quasi-crystalline species. For example, glasses with jadeite like compositions (SAN60) are less durable than those with albite like compositions (SM58). Moreover, it will be shown that the strong relation between the quasi-crystalline species and the cation ratios in a glass can be used to develop a durability model based on activated complex theory (ACT).

5.0 RELATING THE QUASI-CRYSTALLINE SPECIES TO CATION RATIOS

The quasi-crystalline mineral components calculated by NORM-CALC™ for over 300 waste glasses are highly related to the complex cation ratios (Si/Si+Al, Na/Na+B, Na/Na+Li) used by Strachan and Croak [23] and to simple cation ratios such as Al/Si, Fe/Si, Li/B, B/Na, and Mg/Ca used in this study (Figure 3). Figure 3a shows that the glasses modeled with NORM-CALC™ span the composition regions of albite, jadeite, and nepheline rich glasses in terms of their Si/Si+Al and Al/Si cation ratios. Figure 3a also shows that the Si/Si+Al limit of ≥0.7 suggested by Strachan and Croak [23] as the lower durability limit for durable HLW glasses approximately corresponds to the boundary (Si/Si+Al ~ 0.75) between glasses with primarily an albite structure and those with a jadeite structure. The shaded phase boundaries on Figure 3a are determined by the major species calculated for each glass in that phase field, e.g. all the modeling glasses falling between the EA glass and pure albite have positive molar values for albite and/or orthoclase, all of the glasses falling between pure albite and pure jadeite have positive molar values for jadeite, and all of the glasses falling between pure jadeite and pure nepheline have positive molar values for nepheline as indicated in Table 4. In addition, the glasses with low Al/Si ratios in the albite field (see bracket in Figure 3a) have the reedmergnerite structure in which B substitutes for Al in an albite like structure, $NaBSi_3O_8$. Note that the HLW defense glasses including the EA glass and the RX glasses contain either albite or a combination of orthoclase and reedmergnerite structural groups indicating a high degree of silica connectivity.

In terms of the Si/Si+Fe cation ratios and the Fe/Si cation ratios (Figure 3b) the quasi-crystalline mineral structures are somewhat more complex. Pure augite has a composition of $(Ca,Mg)(Al,Fe)_2SiO_6$ and can contain any ratio of Ca:Mg as well as any ratio of Al:Fe. Based on the amount of Al_2O_3 in the augite compositions shown in Figure 3b they are regarded as alumina rich or aluminous augites versus iron rich or ferric/ferrous augites. For the glasses modeled with NORM-CALC™ many glasses contained excess alumina over that used to speciate the alkali-aluminosilicate minerals. Since the ordinate of Figure 3b is the Fe/Si ratio, the more aluminous augites appear at low Fe/Si ratios. Since pure diopside, $(Ca,Mg)Si_2O_6$, another structurally related pyroxene mineral contains no Fe, it also appears at zero Fe/Si. Therefore, a phase field where augite and diopside can co-exist appears at the base of Figure 3b.

The nominal composition of acmite is $NaFeSi_2O_6$ and any iron remaining after NORM-CALC™ speciation as augite is allowed to form acmite. Many of the glasses modeled contained both augite and acmite due to the glass compositions being simultaneously rich in Fe_2O_3, CaO, MgO,

---

compositions. Only a few glasses with high rare-earth concentrations summed to <95 wt% because the rare earth species are not currently considered in NORM-CALC™.

and Na_2O. Therefore, a phase field exists where glasses can be augite and acmite rich in the range of Fe/Si of 0.05 to 0.35. At higher Fe/Si ratios a phase field of glasses containing only acmite exists. Note that the HLW defense glasses including the EA glass and the WCP glasses contain both acmite and augite structural groups indicating a high degree of silica connectivity in the presence of high iron and high sodium. As with Figure 3a, the labeling of the phase fields is consistent with the molar quasi-crystalline species calculated for each glass.

The relation of the cation ratios to the pyroxenes (augite and acmite) is further confounded by the role of the structurally related phase, diopside $(Ca,Mg)Si_2O_6$. The relation of this mineral phase to augite is shown in Figure 3c. The augite at a ratio of Ca:Mg of 1:1 has the same Ca:Mg ratio as diopside if the Ca and Mg cation percents are the same. Therefore, there is a large field shown on Figure 3c where the augites and diopsides overlap and coexist. As with Figure 3a, the labeling of the phase fields is consistent with the molar quasi-crystalline species calculated for each glass.

Boron is first speciated with silica as reedmergnerite, $NaBSi_3O_8$, followed by lithium diborate, $Li_2B_4O_7$ and sodium diborate, $Na_2B_4O_7$. Excess Li is speciated as Li_2SiO_3. Thus the Li/B cation ratios and the B/Na cation ratios are related to these quasi-crystalline phases as indicated in Figure 3d and Figure 3e. As with Figure 3a, the labeling of the phase fields is consistent with the molar quasi-crystalline species calculated for each glass.

6.0 RELATING THE QUASI-CRYSTALLINE SPECIES TO SILICA SATURATION

The quasi-crystalline groups represent the silica connectivity in the glass as modified by the Al, Fe, B, alkaline earths and alkali present, e.g. a reedmergnerite group in the glass creates an activated complex with three silica cations when the associated B cation is exchanged for three protons, an albite group in the glass creates an activated complex with three silica cations when the associated Al cation is exchanged for three protons, and an acmite group in the glass creates an activated complex with two silica groups when the associated Fe cation is exchanged for three protons. Therefore, the molar quasi-crystalline species calculated (see examples in Table 4) should be highly related to the silica-saturation state of the leachates produced by these glasses.

The leachate concentrations shown for the 7-day PCT leachates were converted from mean log Si (ppm) to mean log Si (millimoles/L) by dividing by the molecular weight of Si. Normalized mass loss cannot be used for modeling for this application as it has a composition term in the denominator which confounds the relationship between leachate saturation and glass composition. For the >300 glasses tested by the PCT-A procedure 195 had reported values for which both glass composition and Si leachate data were available. An ordinary least squares regression demonstrated that the silica saturation of the leachates was highly correlated (Figure 4) to all the quasi-crystalline groups by the relationship:

Equation 3 $$\log Si\ (millimoles/L) = -0.22-4.5(Orthoclase)-0.26(Albite)+0.17(Jadeite)+1.5(Nepheline)+2.5(Reedmergnerite)+3.2(Li_2B_4O_7)+1.6(Na_2B_4O_7)+1.3(Acmite)-5.6(Diopside)+1.7(Li_2SiO_3)+4.3(Na_2SiO_3)+2.0(Na_2O)+1.2(Li_2O)$$

The quasi-crystalline relation to solution silica saturation has an R^2 of 0.92 and a RMSE of 0.00968. The F-Ratios and leverage parameters indicate that the strongest influences on the silica saturation of the solution are the amount of sodium disilicate and the amount of excess Na_2O not associated with Si, Al, B, or Fe in other mineral species. These species are the most mobile as they have low connectivity to the other network formers, e.g. Al, B, or Fe, which indicates that

silica saturation is governed by the most mobile alkali species which are liberated first during dissolution and form excess strong bases in solution [78, 79], e.g. NaOH and LiOH. The excess strong bases drive the solution pH more basic in static leach tests. Lithium borate, reedmergnerite, and orthoclase were also determined to have significant leverage effects in Equation 3.

7.0 RELATING THE GLASS QUASI-CRYSTALLINE SPECIES TO GEOCHEMICAL MODELING OF LEACHATES

The >300 glass compositions examined in this study are plotted in Figure 5 against simple cation % ratios and the more complex Strachan and Croak [23] cation ratios. Each figure is shaded to indicate the phases predicted to form from the GWB solution analyses so that the relationship between the quasi-crystalline glass species calculated from NORM-CALC™ can be assessed against the tendency of the solution to form either analcime ($NaAlSi_2O_6 \bullet 1H_2O$), smectite clays such as notronite ($Fe_2O_3{:}2SiO_2 \bullet 2H_2O$) or kaolinite ($Al_2O_3{:}2SiO_2 \bullet 2H_2O$), or paragonite clays ($NaAl_3Si_3O_{10}(OH)_2$). Figure 5 compares the 1 week leachate predictions (top) to the 4 week predictions (middle) and also to the 24 week leachate predictions (bottom).

In Figure 5a (top) the 1 week leachate data indicate that glasses with primarily albite quasi-crystalline groupings form leachates that are saturated with respect to ferrite phases like FeOOH (goethite) and/or notronite, Fe-rich clays. These glasses are often also enriched in the boron substituted albite phase known as reedmergnerite. The field of potential analcime precipitation from the leachate compositions occurs in glasses that are predominately jadeite quasi-crystals. Jadiete can easily form analcime via the following reaction:

Equation 4 $$NaAlSi_2O_6 + H_2O \rightarrow NaAlSi_2O_6 \bullet H_2O$$
jadeite *analcime*

which has a -9.8 kJ/mole free energy of formation at 90°C. Note that the Al:Si ratio of jadeite and analcime are the same, e.g. analcime is hydrated jadeite.

The potential analcime precipitation region overlaps part of the albite region of quasi-crystals, e.g. to an Al/Si ratio of ~0.2. That is because analcime exists as a solid solution ranging from natrolite (see Figure 5a) of $NaAlSi_{1.5}O_5 \bullet 0.75H_2O$ on the high Al side of stoichiometric analcime ($NaAlSi_2O_6 \bullet H_2O$) to $NaAlSi_3O_8 \bullet 1.5H_2O$ on the low Al side [109] as shown in Figure 5.

The nonstoichometric analcime known as natrolite has an Al:Si ratio of 1:1.5 close to that of nepheline, while stoichiometric analcime has the same Al:Si ratio as jadeite, and the $NaAlSi_3O_8 \bullet 1.5H_2O$ composition of analcime has the Al:Si ratio of albite. However, thermodynamic data are only available for stoichiometric analcime and so the relative thermodynamic driving force for analcime derived from albite, jadeite, and nepheline can only be estimated from the available data. For example, the conversion of albite to analcime is not energetically favored at 90°C via the reaction

Equation 5 $$2NaAlSi_3O_8 + H_2O \rightarrow NaAlSi_2O_6 \bullet H_2O + SiO_2\ (aq)$$
albite *analcime*

which has a positive 23.5 kJ/mole free energy of formation at 90°C while Equation 4 demonstrates that analcime can readily form from jadeite. This indicates that the stoichiometry of the jadeite quasi-crystalline groups having an Al:Si ratio of 1:2 controls the activated complexes which release Al:Si to solution in ~1:2 ratio. This is exactly the stoichiometric ratio of Al to Si needed in the leachate for it to be saturated with respect to analcime.

In the quasi-crystalline region of Figure 5a that corresponds to nepheline, paragonite clays along with some other zeolites (laumontite), $Al(OH)_3$ (gibbsite) and kaolinite form. Paragonite with an Al: Si ratio of 1:1 probably cannot form directly from nepheline quasi-crystalline groups even though nepheline and paragonite both have the same Al:Si ratio because the following reaction

Equation 6 $3NaAlSiO_4 + 2H_2O \rightarrow NaAl_3Si_3O_{10}(OH)_2 + 2NaOH$
nepheline *paragonite*

is not energetically favored, it has a positive 39.2 kJ/mol free energy of formation at 90°C.

However, the formation of paragonite from nepheline is favored if the solution is slightly acidic, e.g. -139 KJ/mol free energy of formation (Equation 7):

Equation 7 $3NaAlSiO_4 + 2H^+ \rightarrow NaAl_3Si_3O_{10}(OH)_2 + 2Na^+$
nepheline *paragonite*

or if the leachant solution becomes more basic, e.g. when Na_2O in the glass hydrolyses and releases OH^- then.

Equation 8 $3NaAlSiO_4 + OH^- \rightarrow NaAl_3Si_3O_{10}(OH)_2 + 2Na^+$
nepheline *paragonite*

If the solution continues to become more basic during static leachate testing and the SiO_2(aq) concentration in the solution also increases then the solutions that are saturated with paragonite can easily become saturated with respect to analcime (Equation 9). The free energy of the aging conversion, which is in agreement with the paragenic sequences observed experimentally [52,53] by is -170 kJ/mol at 90°C.

Equation 9 $NaAl_3Si_3O_{10}(OH)_2 + 2NaOH\ (aq) + 3SiO_2\ (aq) \rightarrow 3NaAlSi_2O_6 \bullet H_2O + H_2O$
paragonite *analcime*

This is shown graphically in Figure 7 where the fields of analcime and paragonite overlap each other on the activity (stability) diagram of log activity Na^+/H^+ vs log activity SiO_2 (aq). If one mineral is suppressed during calculation of the stability diagram the other phase field is superimposed in the same leachate composition space.

In addition, analcime can also form directly from nepheline in the presence of excess SiO_2(aq) and no increase in the solution pH (Equation 10). This reaction has a free energy of formation of -38.2 kJ/mole at 90°C.

Equation 10 $3NaAlSiO_4 + SiO_2(aq) + H_2O \rightarrow NaAlSi_2O_6 \bullet H_2O$
nepheline *analcime*

Equation 9 and Equation 10 explain the zonation of the leached layers observed on waste glasses during examination by transmission electron microscopy and the transformation sequences observed

Unaltered glass → smectite clays (e.g. paragonite) → analcime

that mimic the geologic deposition sequences exhibited by mineral deposits in lacustrine basins as the solutions become more caustic [52,53].

Figure 5a indicates that the Al:Si ratio of glasses should be limited to ~0.2 to avoid analcime precipitation from glasses containing nepheline, jadeite, and albite quasi-crystalline groups. This ratio corresponds to a Si/Si+Al ratio of ~0.825 and is in disagreement with the ratio of Si/Si+Al of 0.7 suggested by Strachan and Croak [23].

It is of interest to examine the position of the two glasses studied by Van Isenghem and Grambow [20] in Figure 5. The SAN 60 glass that forms analcime on its surface and causes the glass to exhibit Stage III leachate behavior, has the exact Al:Si ratio of jadeite and is calculated to form primarily all jadeite quasi-crystals (Table 4). The SM-58 glass on the other hand is calculated to form primarily albite quasi-crystalline groups (Figure 5a, Table 4). It should also be noted that the WCP and EA glasses, high iron defense waste glasses, tend to form albite quasi-crystals. All of the high iron defense waste glasses and SM58 also form either ferrites and/or Fe-rich clays such as notronites during GWB modeling (Figure 5a) and have Fe-rich quasi-crystals such as acmite-augites and/or hematite (Fe_2O_3).

In Figure 5b, the 4 week durability data indicates an even stronger correlation between glasses that are primarily composed of jadeite quasi-crystals with an Al:Si ratio of 1:2 and leachates that are saturated with respect to the precipitation of analcime with a similar stoichiometric ratio. However, the leachate saturation field of paragonite, kaolinite, and gibbsite has now become a leachate field saturated with respect to analcime and paragonite and the leachates saturated with both these phases extends from the natrolite composition in the nepheline quasi-crystalline field to 0.2 Al/Si in the albite quasi-crystalline field. The leachate pH values of the 4 week durability tests are more basic than the leachate pH values for the corresponding 1 week durability tests for all the glasses studied. As shown in Equation 8 and Equation 9, paragonite in the presence of excess NaOH with or without increasing SiO_2(aq) in the leachate can readily transform to analcime.

In Figure 5c the glasses tested for 24 weeks are plotted. It is of significance that now there are only two leachate saturation phase fields, one for ferrites and one for analcime. This indicates that all of the leachates that were saturated with respect to other aluminates such as gibbsite or aluminosilicates such as paragonite, laumontite, kaolinite, and/or lawsonite have converted to analcime except for the high-iron containing defense waste glasses and the French SM58 which is low in Al and has Fe as a component. The leachate pH values of the 24 week durability tests are more basic than the leachate pH values for the corresponding 4 week durability tests for all the glasses studied. Figure 5c indicates that glasses with an Al/Si ratio greater than 0.2 will be prone to form analcime and potentially return to Stage III leachate behavior as observed for the French SAN60 glass.

The ferrite phases predicted to be saturated in the 24 week leachates (Figure 5c) are primarily notronite and/or goethite (FeOOH). The glasses saturated with respect to notronite in Figure 5

have albite quasi-crystalline groups but also have either acmite or augite quasi-crystalline groups (Table 4). For example, the French SM58 glass contains both augite and hematite as a source of iron for notronite formation while the EA and the WCP glasses contain acmite, augite and hematite. If the thermodynamics of formation of notronite from albite and acmite is examined (Equation 11) the free energy of formation is -604 kJ/mol at 90°C. Likewise, the formation of notronite from a mixture of acmite and jadeite and/or acmite and nepheline has free energy of formation values of -624.36 kJ/mol and -611.75 kJ/mole, respectively.

Equation 11

$$2NaFeSi_2O_6 + 0.33NaAlSi_3O_8 + 2H_2O \rightarrow Na_{0.33}Fe_2Al_{0.33}Si_{3.67}O_{10}(OH)_2 + 1.32SiO_2(aq) + 2NaOH$$

acmite *albite* *notronite*

Notronite is likely the favored hydrated form of the aluminous augite quasi-crystalline groups formed in many of the glasses modeled (Figure 3) although thermodynamic data for the aluminous augites are not available. Therefore, the presence of acmite and/or augite groups appears to stabilize the formation of notronite rather than analcime and prevents the formation of Stage III leaching behavior.

8.0 RELATING QUASI-CRYSTALLINE ATOMIC RATIOS TO SHORT TERM DURABILITY

The quasi-crystalline groups in a glass have been shown to be a measure of the polymerization of the glass and related to the leachate silica saturation. In addition, it has been shown that there is a structural relation between the alkalis and boron, the alkalis and silica, and the alkalis to Al and Fe. These structural stoichiometric ratios are correlated to the stoichiometry of the activated complexes that form on the surface by the law of mass action and thus control the stoichiometry of the phases that form on the glass surface, e.g. analcime vs. clays, and in the solution. A relationship was also demonstrated between simple cation ratios and the quasi-crystalline mineral groupings (Figure 3) demonstrating how alkali and alkaline earths are distributed amongst the network formers, B, Si, Al, and Fe.

Therefore, a glass durability model can be developed to simply and adequately determine glass durability relative to a standard glass such as the Environmental Assessment (EA) glass based on the relationship of simple ratios to both glass structure and the stoichiometry of the activated complexes that mechanistically relate the concentrations of all the species released to the leachate solution. These simple ratios should be useful for process control and for formulating durable glasses for the HLW disposal environment.

The structural ratio durability models are linear in the unknown coefficients[f] and highly accurate (R^2 = 0.89-0.94) for over 300 glasses of wide composition ratios (Figure 8). These models were developed based on the 7 day durability test data given in

[f] but non-linear in glass composition like other process models that have been implemented at the Savannah River Site Defense Waste Processing Facility

Table 2. The same seven cation ratios are used in each model, i.e., Al/Si, Fe/Si, Al/Fe, Al/B, ΣAlkali/Si, ΣAlkali/B, and ΣAlkali/(Al+Fe) where Σalkali is K_2O+Na_2O+Li_2O. These ratios represent the distribution of the alkalis and alkaline earths amongst the network forming cations, e.g. Al/Si represents the partitioning of the Al among the potassium and sodium aluminosilicates (orthoclase, albite, jadeite, and nepheline), the Fe/Si represents the partitioning of the Fe among the pyroxenes (acmites and augites), Al/B represents the role of reedmergnerite ($NaBSi_3O_8$) versus albite ($NaAlSi_3O_8$), the ΣAlkali/Si represents the role of $(Na,Li)_2SiO_3$, the ΣAlkali/B represents the role of $(Na,Li)_2B_4O_7$, and the ΣAlkali/(Al+Fe) represents the role of the alkali aluminosilicates and the alkali pyroxenes.

The coefficients in each equation vary depending on the leachate species being modeled:

Equation 12 log Na (millimoles/L) = -3.88 – 1.74Al/Si + 7.53 Fe/Si - 0.05Al/Fe +1.13Al/B + 0.63Alk/Si – 0.25Alk/B + 0.93Alk/Al+Fe

Equation 13 log B (millimoles/L) = -2.34 – 1.27Al/Si + 3.94Fe/Si – 0.02Al/Fe + 0.15Al/B + 0.84Alk/Si – 0.26Alk/B + 0.68Alk/Al+Fe

Equation 14 log Li (millimoles/L) = -1.13 – 2.83Al/Si + 0.47Fe/Si - 0.03 Al/Fe + 0.46 Al/B + 1.28Alk/Si – 0.12Alk/B + 0.34 Alk/Al+Fe

Equation 15 log Si (millimoles/L) = -1.20 – 0.44Al/Si + 2.51Fe/Si + 0.02Al/Fe + 0.10 Al/B + 0.26Alk/Si - 0.07Alk/B + 0.47 Alk/Al+Fe

Figure 6 indicates that these same ratios can be plotted on ternary diagrams to illustrate glasses low in Al/Si at constant ratios of Fe/Si and Alkali/Al+Fe can be used to distinguish glasses that form ferrites (notronite clays) from glasses that form analcime. This is also illustrated in a different ternary representation of Mg/Ca vs. Al/Si vs. alkali/B. Therefore, a durability model based on atomic ratios is capable of distinguishing the quasi-crystalline mineral groups in a glass, the silica saturation, and the saturation of the leachates with respect to clays versus analcime. The durability model can also be used to predict the PCT response necessary for compliance with the Waste Acceptance Product Specifications (WAPS) relative to a benchmark standard glass like the Environmental Assessment (EA) glass in the same manner as existing HLW glass durability models. The ability to predict the return to the forward rate is also of interest to the Performance Assessments (PA) conducted for shallow land burial of LAW glasses.

9.0 CONCLUSIONS

The most important requirement for high-level waste (HLW) glass acceptance for disposal in a geological repository is the chemical durability, expressed as a glass dissolution rate. The formation of clay mineral assemblages on the leached glass surface causes the dissolution rate to slow to a long-term “steady state” rate. The formation of zeolite mineral assemblages specifically analcime ($NaAlSi_2O_6 \bullet H_2O$) on leached glass surface layers causes the dissolution rate to increase

and return to the initial high forward rate. The return to the forward dissolution rate is undesirable for long-term performance of glass in a disposal environment.

A method of calculating the quasi-crystalline mineral groups for over 300 glasses from their composition was developed. The basis for the quasi-crystalline modeling was the methodology of Cross-Iddings-Pirsson-Washington or C.I.P.W. calculation, for determining the mineral species that would form from a natural glass if it were to slowly crystallize. The C.I.P.W normative calculations are based on the known principles of mineral crystallization from molten magmas, e.g. natural glasses. Adaptations had to be made for the boron species in HLW glasses that are not normally present in natural magmas and glasses.

The quasi-crystalline mineral groups were shown to be related to the silica saturation of the leachates and to simple ratios of glass cation components like Al/Si and Si/Al+ Si. The leachates of the over 300 glasses leached for 1 week, 4 weeks, and 24 weeks in deionized water and J13 Yucca Mountain repository water were analyzed using Geochemists Work Bench (GWB) Version 4.0.

The saturation of the leachates with respect to clays, ferrites, and analcime was assessed with the atomic ratio approach. The phases predicted by GWB were overlain on the quasi-crystalline ratio diagrams and demonstrated that glasses that were primarily albite structured with some reedmergnerite borate groups were extremely durable. If these glasses also contained sufficient iron to form either acmite or aluminous augite quasi-crystalline groups then ferrite clay (notronite) would form on the leached surface layer instead of analcime. In terms of cation ratios glasses should contain Al/Si ratios of ≤ 0.2 and some iron so that notronite forms instead of analcime. This will prevent or retard glasses from exhibiting Stage III behavior.

This provides two different methods by which a glass durability model can be formulated. One based on the quasi-crystalline mineral species in a glass and one based on cation ratios in the glass: both are related to the activated complexes on the surface by the law of mass action. The former would allow a Thermodynamic Hydration Energy MOdel (THERMO™) to be developed based on the hydration of the quasi-crystalline mineral species if all the pertinent thermodynamic data were available. Since the pertinent thermodynamic data is not available, the quasi-crystalline mineral species and the activated complexes can be related to cation ratios in the glass by the law of mass action. The cation ratio model can, thus, be used by waste form producers to formulate durable glasses based on fundamental structural and activated complex theories. Moreover, a glass durability model based on atomic ratios simplifies HLW glass process control in that the measured ratios of only a few waste components and glass formers can be used to predict complex HLW glass performance with a high degree of accuracy, e.g. an R^2~0.97.

10.0 ACKNOWLEDGEMENTS

The authors would like to gratefully acknowledge the assistance of Troy Lorier of Savannah River National Laboratory in helping compile the glass durability databases.

This paper was prepared in connection with work done under Contract No. DE-AC09-96SR18500 with the U.S. Department of Energy (DOE). Specifically, this research was supported in part by an Independent Research & Development (IR&D) grant from the Savannah River National Laboratory and by the DOE Tank Focus Area (TFA) Technical Task Plan #SR-16WT-31, Subtask F.3.

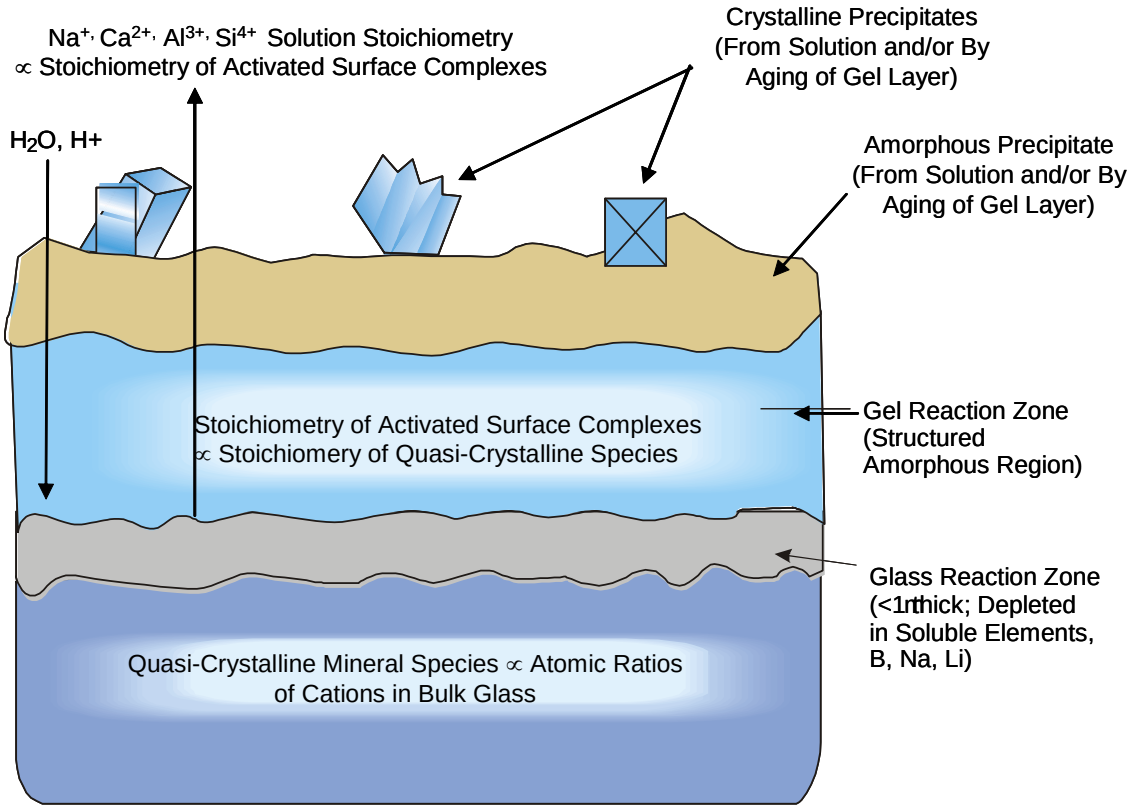

Figure 1. Schematic relationship between the stoichiometry of the parent glass, the activated surface complexes, and the leached layer-solution chemistry.

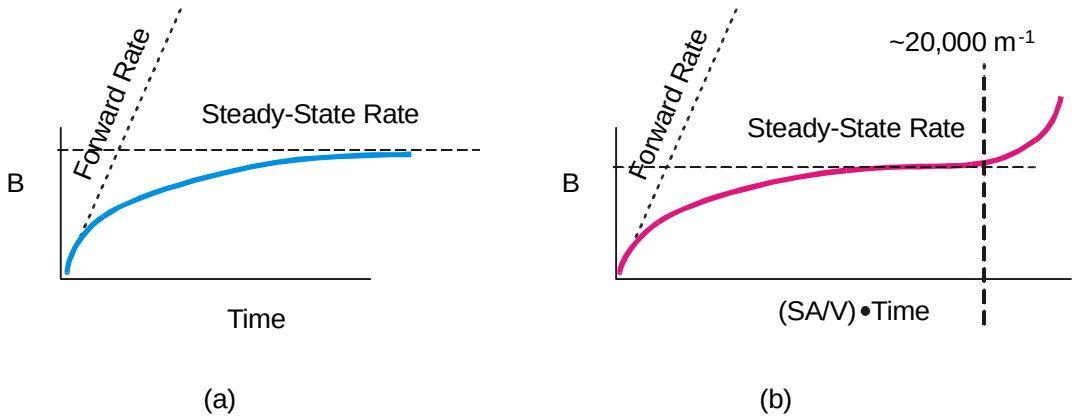

Figure 2. (a) Parabolic behavior of the diffusion of a soluble species out of the glass through an increasingly thick surface layer [28] (b) Acceleration of glass durability tests using glass surface area (SA), leachant volume (V), and time. Acceleration appears to follow parabolic diffusion kinetics until ~20,000 m^{-1} when the glass dissolution mechanism appears to change reverting to the forward rate.

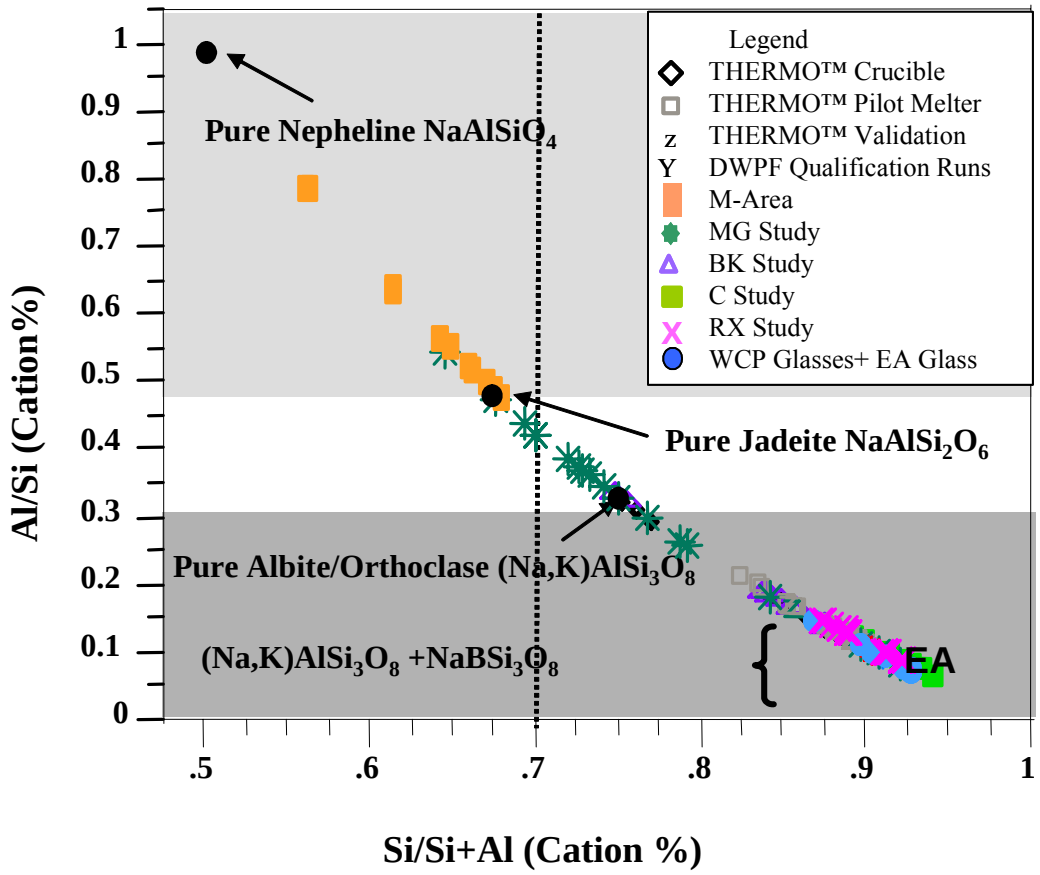

Figure 3a Relation of simple ratios (Al/Si, Fe/Si, Mg/Ca, B/Na, Li/B) to complex ratios used by Strachan and Croak [23] and to calculated quasi-crystalline mineral species for >300 simulated waste glasses.

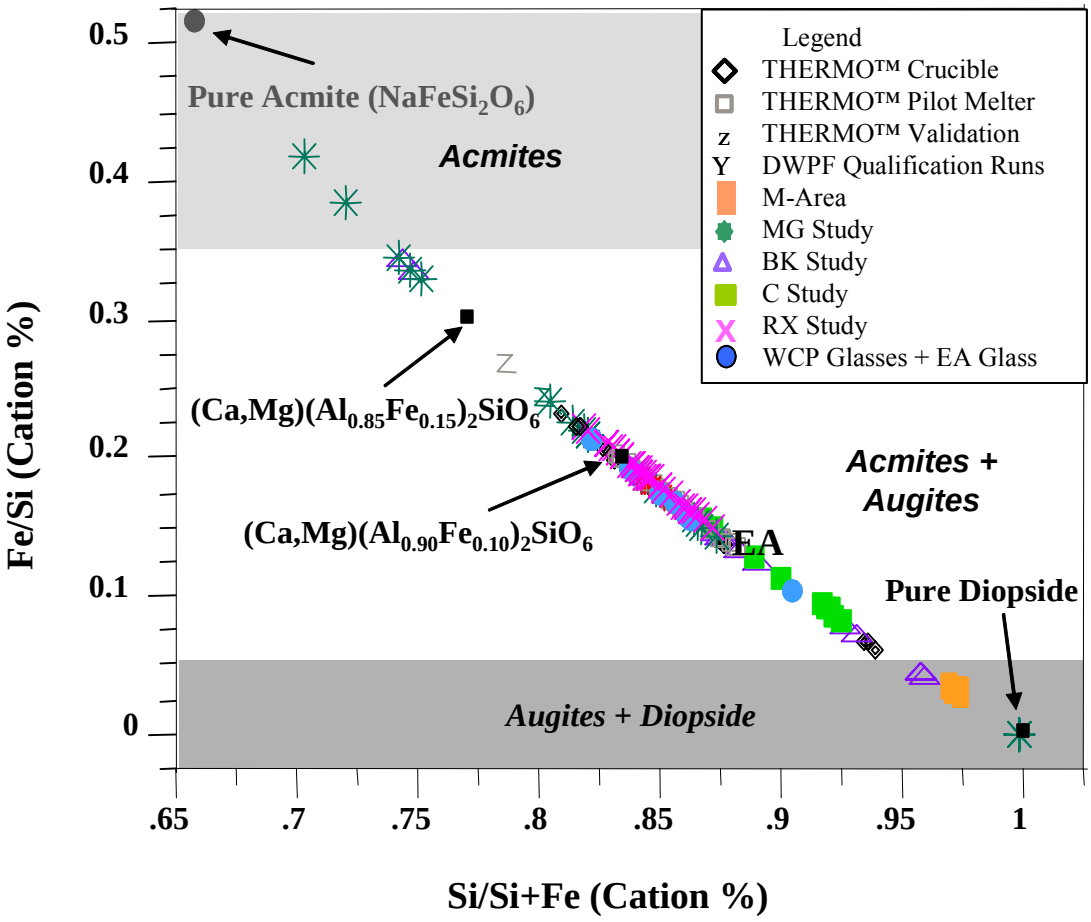

Figure 3b. Relation of simple ratios (Al/Si, Fe/Si, Mg/Ca, B/Na, Li/B) to complex ratios used by Strachan and Croak [23] and to calculated quasi-crystalline mineral species for >300 simulated waste glasses.

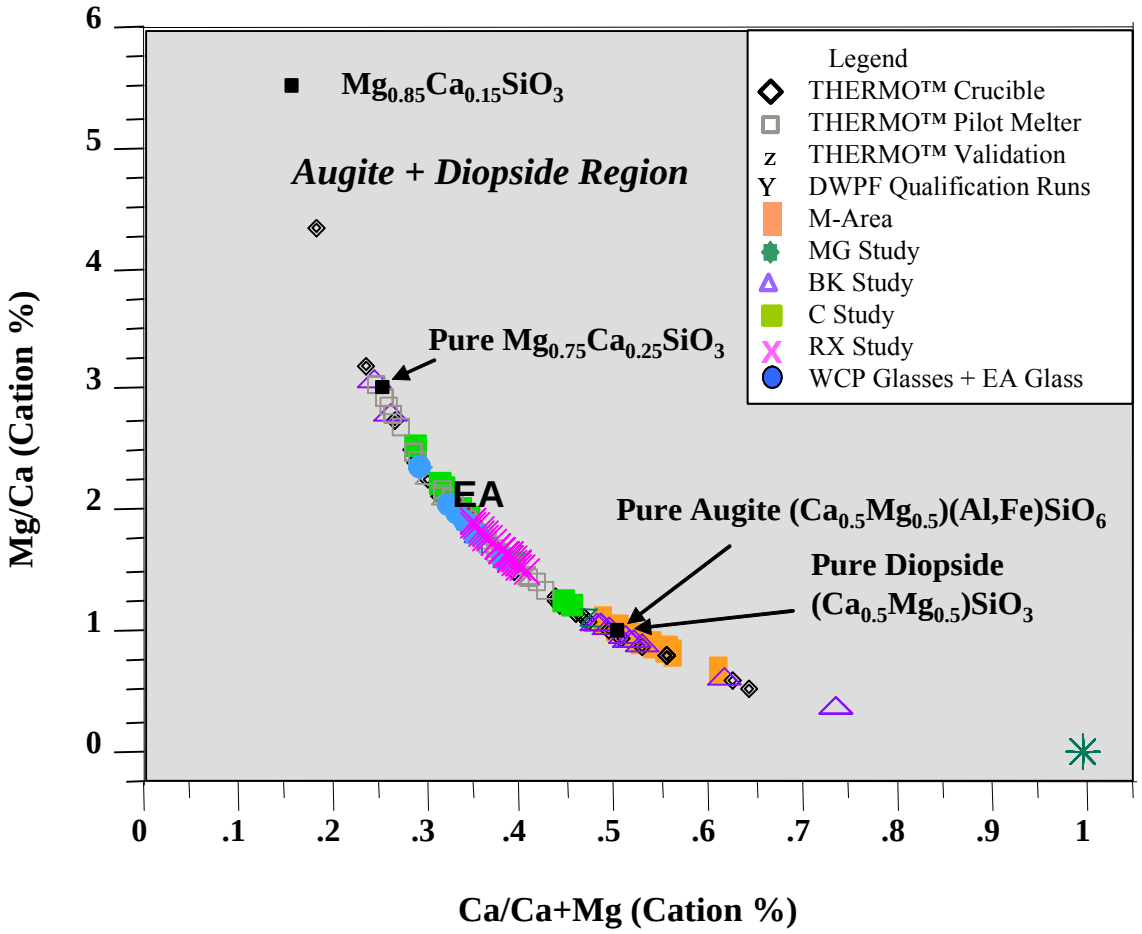

Figure 3c. Relation of simple ratios (Al/Si, Fe/Si, Mg/Ca, B/Na, Li/B) to complex ratios used by Strachan and Croak [23] and to calculated quasi-crystalline mineral species for >300 simulated waste glasses.

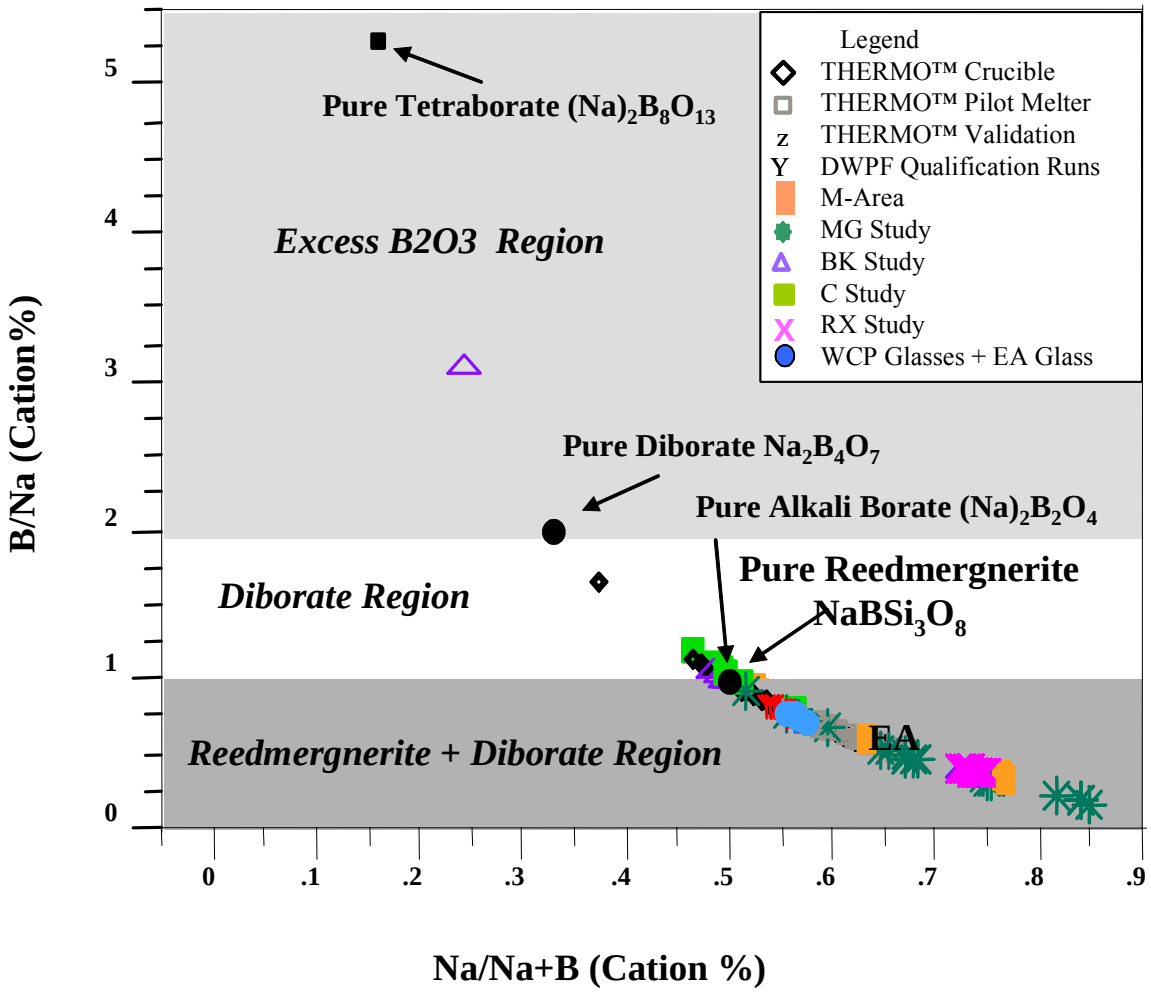

Figure 3d. Relation of simple ratios (Al/Si, Fe/Si, Mg/Ca, B/Na, Li/B) to complex ratios used by Strachan and Croak [23] and to calculated quasi-crystalline mineral species for >300 simulated waste glasses.

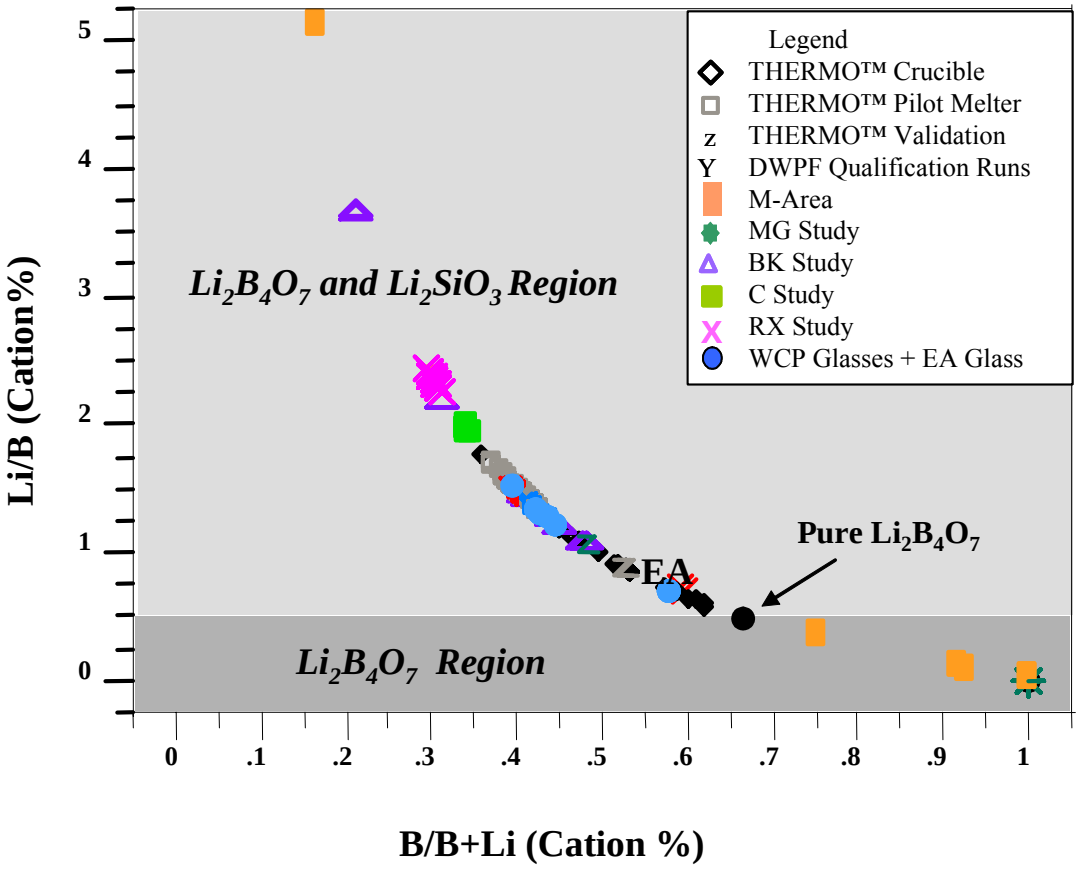

Figure 3e. Relation of simple ratios (Al/Si, Fe/Si, Mg/Ca, B/Na, Li/B) to complex ratios used by Strachan and Croak [23] and to calculated quasi-crystalline mineral species for >300 simulated waste glasses.

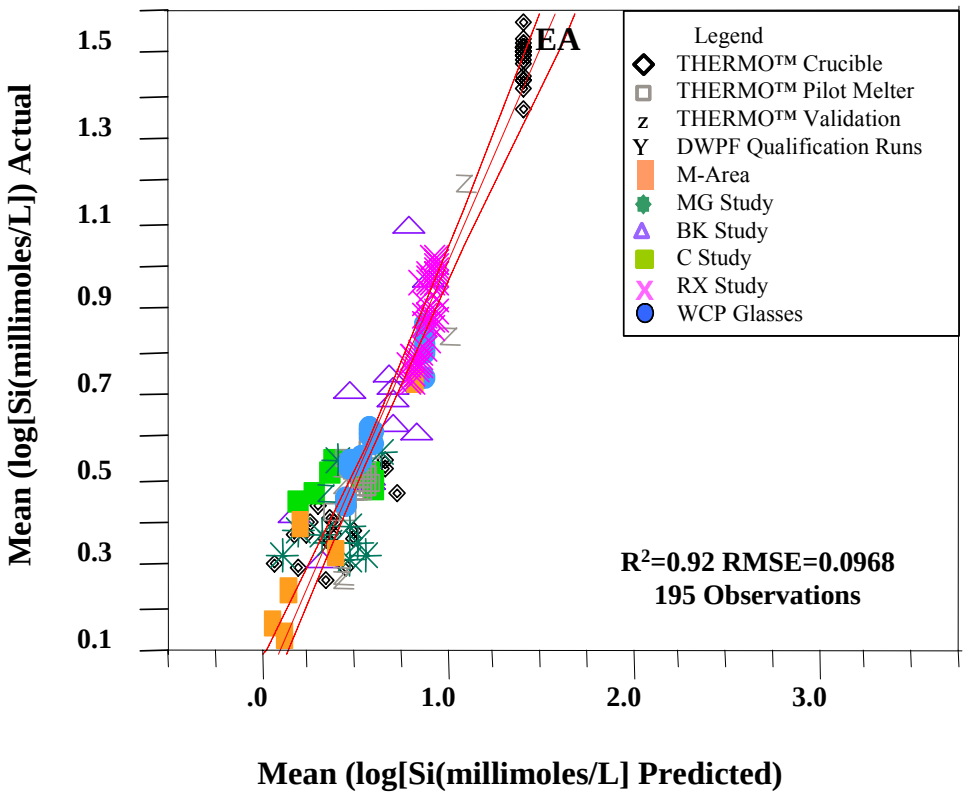

Figure 4. Relation of the leachate silica saturation to the quasi-crystalline groups as given in Equation 3.

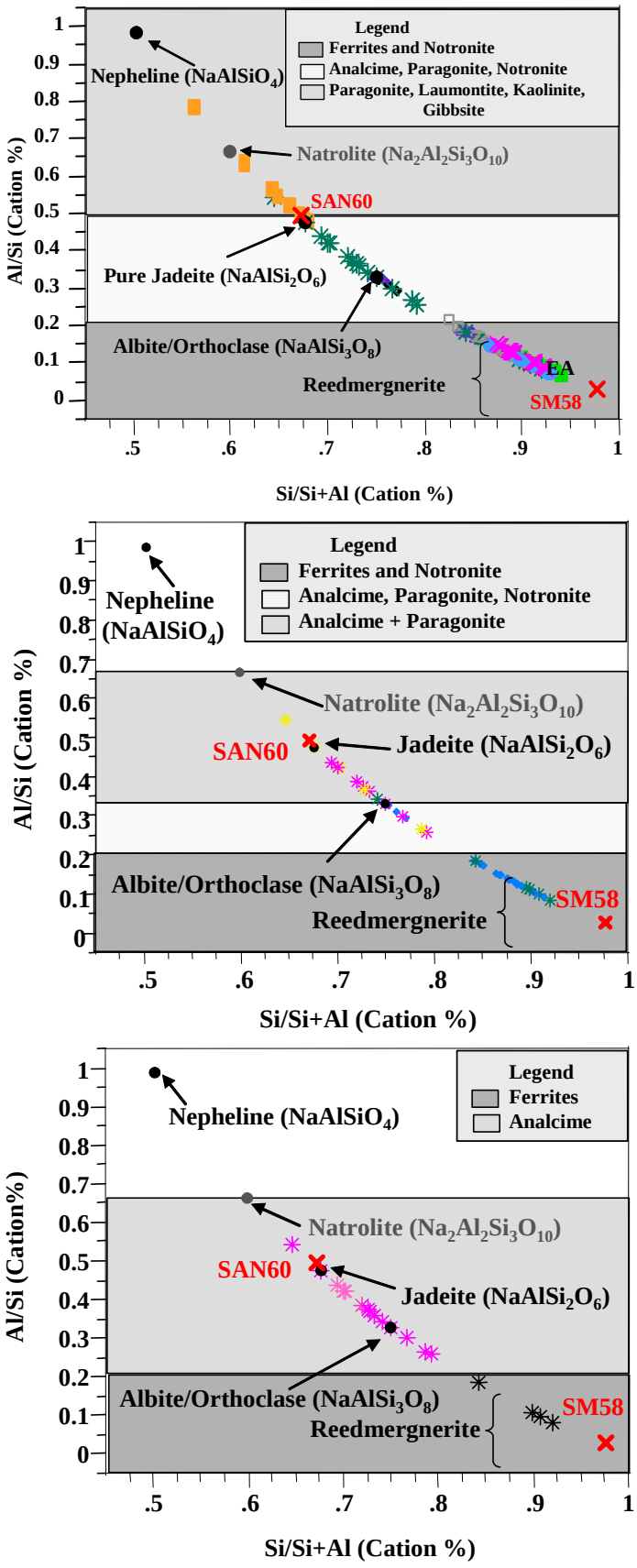

Figure 5. Prediction of analcime formation from cation ratios by superimposing the phase fields predicted from GWB based on 1 week (top), 4 week (middle), and 24 week (bottom) PCT leachate data.

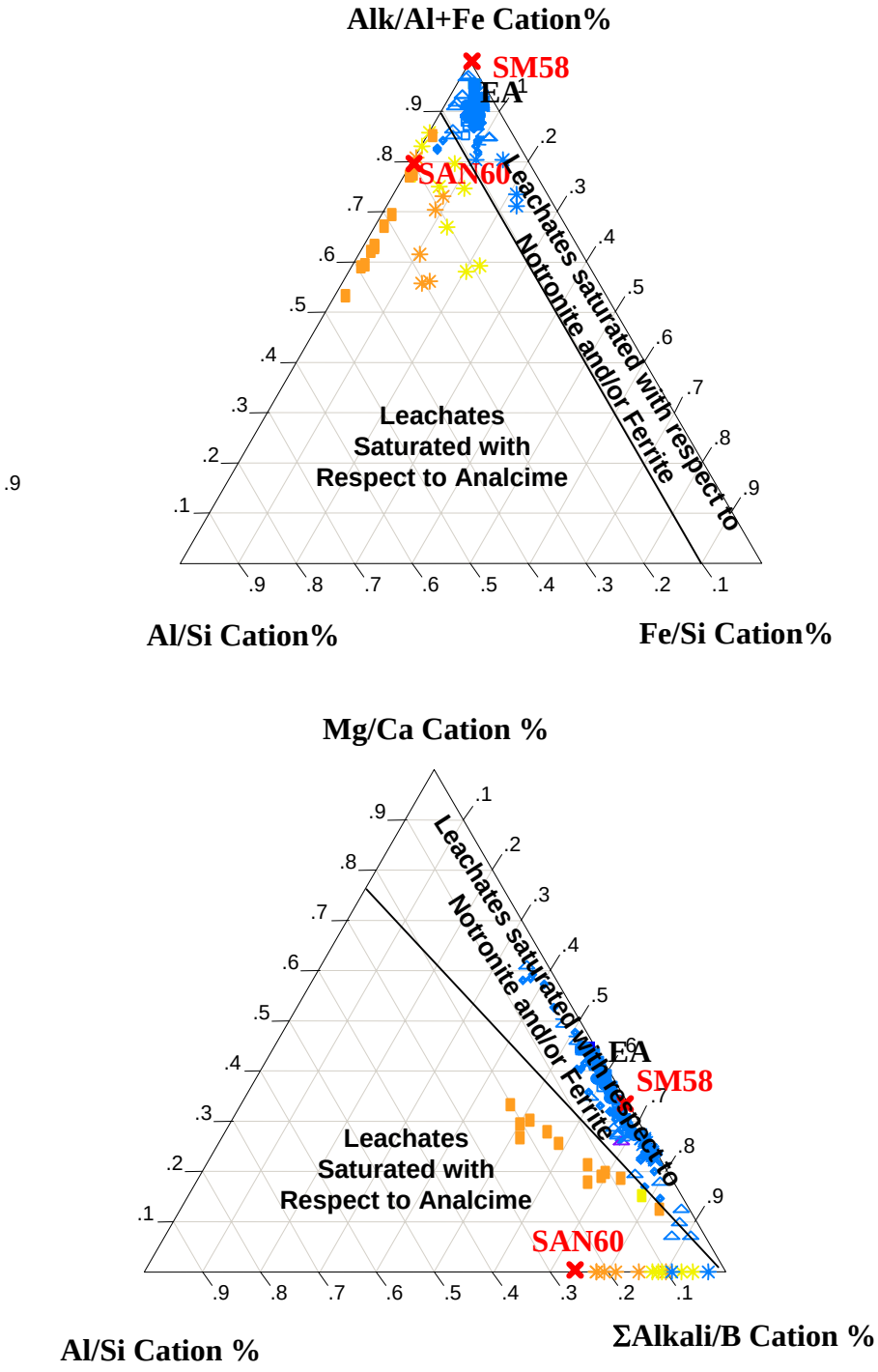

Figure 6. Ternary diagrams demonstrating how the cation ratios define the fields of glasses that have a tendency to form analcime (region including SAN60 glass) from the glasses that have a tendency to form ferrites and notronites (region including SM58 and defense waste glasses).

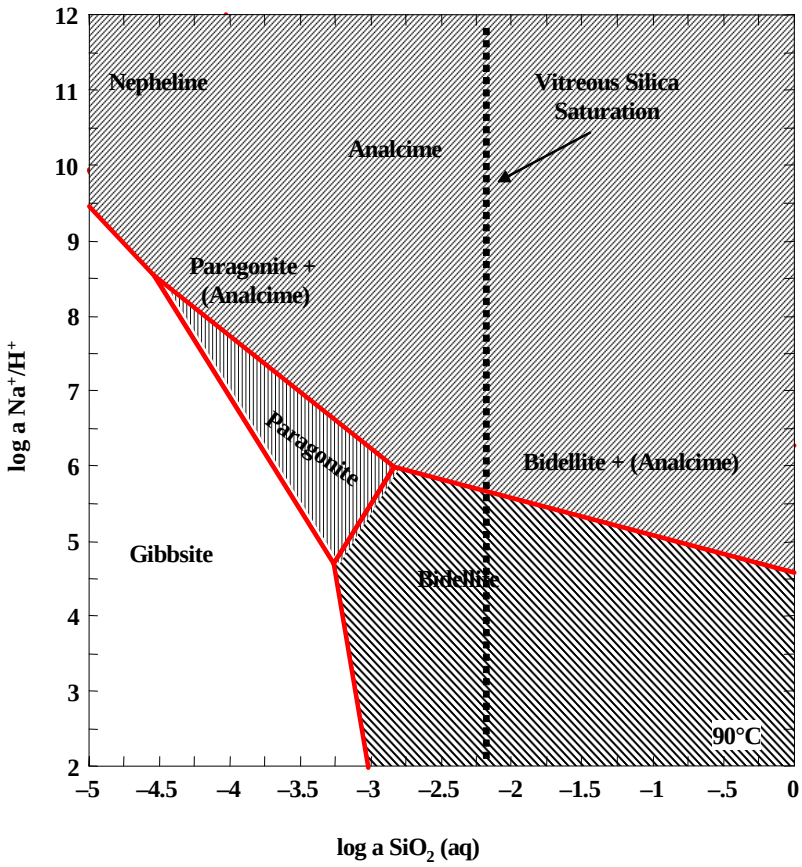

Figure 7 Prediction of analcime formation from cation ratios by superimposing the phase fields predicted from GWB based on 4 week PCT leachate data.

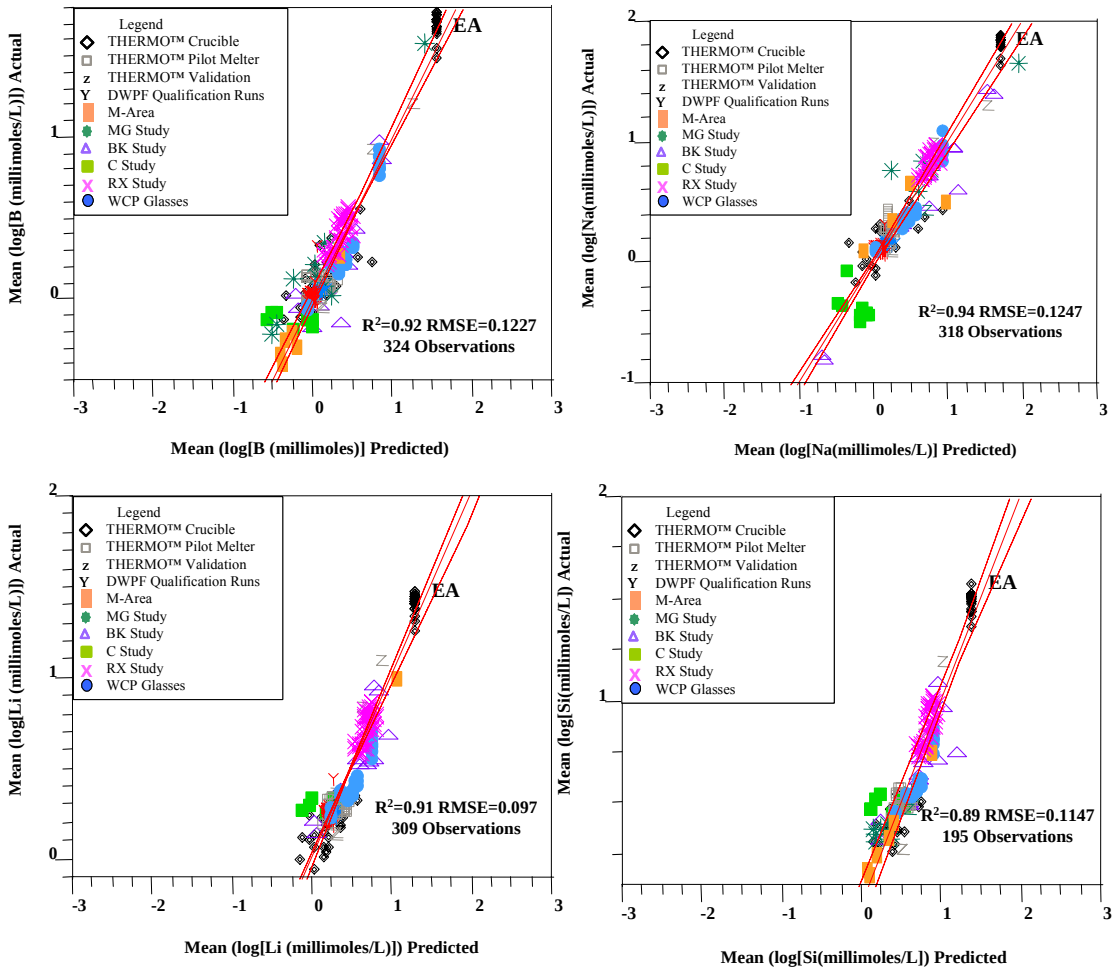

Figure 8a. Relation of the leachate species i given in log i (millimoles/L) from 7-day PCT Durability Testing to the structural ratios Al/Si, Fe/Si, Al/Fe, Al/B, Alkali/B, Alkali/Si and Alkali/(Al+Fe) given by Equation 12 to Equation 15 . Data for >300 glass durability (tests performed in triplicate) are shown.

Table 1. Glass Durability Studies Considered During Modeling

Study	Number of Glasses	Laboratory Performing Glass Measurements	Technique Used to Determine Glass Homogeneity	Number of 7 day Tests	Number of >7 day Tests	Ref.
THERMO™ Crucibles	35	SRNL –ADS	XRD, SEM, TEM	105 Teflon®	62 Teflon®	78,79
THERMO™ Pilot Scale and Startup Frit	41	SRNL –ADS	XRD, SEM, TEM	123 Teflon®	0	78,79
THERMO™ Validation*	27	SRNL –ADS	XRD, SEM, TEM	81 Teflon® and Stainless Steel	0	78,79
DWPF Qualification (grab, canister and wall)	125	SRNL –ADS	XRD	375 Stainless Steel	0	78,79
WCP Glasses	7	CELS	XRD, SEM, TEM	63 Teflon® and Stainless Steel	0	79, 80,81
EA Glass	1	CELS	XRD, SEM, TEM	57 Teflon® and Stainless Steel	0	79, 82,83
SRS M-Area	31	SRNL –ADS	XRD	62 Teflon®	0	84
MG Study	33	SRNL –ADS and CELS	XRD, SEM, TEM	99 Teflon®	261 (DI water in Teflon®) 54 (J-13 water in Teflon®)	72
BK Study	28	SRNL –ADS	UNKNOWN	84 Stainless Steel	0	73
C Study	46	SRNL –ADS	XRD, SEM, TEM	138 Stainless Steel	0	74
R Study	24	SRNL –ADS	XRD	72 Stainless Steel	0	75
REE Study	54	SRNL –ADS	XRD	162 Stainless Steel	0	76
RX Study	45	SRNL-ML	VISUAL	135 Stainless Steel	0	77

*Excluding MG, BK, C, R, REE and Qualification Runs

Table 2. Oxide Ranges of Model Glasses Compared to those of Van Isenghem and Grambow [20]

Sample	MAX	MIN	SM58	SAN60
Al_2O_3	25.04	2.99	1.20	18.10
B_2O_3	13.65	3.48	12.30	17.00
BaO	0.25	0.00	0.00	0.00
CaO	8.68	0.00	3.80	3.50
Ce_2O_3	0.14	0.00	0.00	0.00
Cr_2O_3	0.86	0.00	0.00	0.00
Cs_2O	0.12	0.00	0.00	0.00
CuO	0.26	0.00	0.00	0.00
Cu_2O	0.23	0.00	0.00	0.00
FeO	3.99	0.00	0.00	0.00
Fe_2O_3	20.77	0.00	1.20	0.30
K_2O	4.81	0.00	0.00	0.00
La_2O_3	0.42	0.00	0.00	0.00
Li_2O	11.15	0.00	3.70	5.00
MgO	1.86	0.00	2.00	0.00
MnO	5.09	0.00	0.00	0.00
MoO_3	0.22	0.00	0.00	0.00
Na_2O	24.43	2.84	8.30	10.70
Nd_2O_3	0.67	0.00	0.00	0.00
NiO	1.77	0.00	0.00	0.00
P_2O_5	3.08	0.00	0.00	0.00
PbO	0.25	0.00	0.00	0.00
SiO_2	68.50	37.79	56.90	43.40
SrO	0.16	0.00	0.00	0.00
TiO_2	1.71	0.00	4.40	0.00
U_3O_8	5.66	0.00	0.00	0.00
ZnO	0.44	0.00	0.00	0.00
ZrO_2	1.25	0.00	0.00	0.00
Fission Products and Actinides	N/A	N/A	6.20	2.0
Oxide Sum	104.28	95.08	100.00	100.00

Table 3. Ranges of Cation% Ratios for Model Glasses Compared to those of Strachan and Croak [23]

Cation% Ratios	SM58	SAN60	Ref 23 MAX	Ref 23 MIN	MAX	MIN
Si/Si+Al	0.98	0.67	1.00	0.55	0.94	0.56
Na/Na+B	0.43	0.41	1.00	0.2	0.85	0.24
B/B+Li	0.59	0.59	1.00	0	1.00	0.16
Na/Na+Ca	0.80	0.85	1.00	0.2	1.00	0.71
Fe/Fe+(Ca+Mg)	0.11	0.06	N/A	N/A	1.00	0.00
Na/Na+Li	0.52	0.51	1.00	0.2	1.00	0.21
Si/Si+Fe	0.98	0.99	N/A	N/A	1.00	0.70
Na/Na+Fe	0.94	0.00	N/A	N/A	1.00	0.00

Table 4. Quasi-Crystalline Species (Mole%) For Selected Glasses Studied

Mineral Species (Moles)	SM58	SAN60	EA	WCP Batch 1	WCP HM	WC P PX	MG-15	MG-16	MG-19	MG-2	MG-21	MG-22	MG-24	MG-25	MG-26	MG-27	MG-28	MG-29	MG-31	MG-32	MG-33	MG-4	MG-6	MG-8	MAX
Orthoclase			0.072	0.071	0.047	0.059																			0.102
Albite	0.024			0.025	0.093				0.075		0.217		0.144	0.253	0.216			0.223					0.083	0.071	0.263
Jadeite		0.345					0.334	0.292		0.311						0.279	0.283		0.279	0.308	0.343	0.329			0.343
Nepheline												0.358													0.467
Reedmergnerite			0.162																					0.133	0.218
$Li_2B_4O_7$	0.177	0.244		0.112	0.101	0.148																			0.191
NaB_4O_7							0.068	0.059	0.190	0.074	0.124	0.134	0.149	0.196	0.062	0.114	0.131	0.104	0.108	0.074	0.122	0.064	0.183		0.196
Acmite			0.056	0.047		0.057		0.052	0.222		0.009	0.011	0.014	0.002	0.015		0.099	0.011	0.009		0.017		0.127	0.011	0.222
Hematite (Fe_2O_3)	0.008	0.002	0.056	0.057	0.049	0.054		0.107	0.029		0.055	0.073	0.081	0.058	0.081	0.057	0.034	0.122	0.051	0.079	0.056		0.076	0.131	0.131
Augite	0.008	0.007	0.006	0.057	0.049	0.054					0.055	0.073	0.081		0.081	0.057		0.047	0.051	0.074				0.131	0.131
Diopside	0.110		0.061		0.006																				0.060
Li_2SiO_3	0.036		0.235	0.092	0.104	0.034																			0.337
Na_2SiO_3	0.122		0.228	0.109	0.091	0.182				0.036	0.094	0.004	0.121			0.052						0.168			0.235
Excess SiO_2	0.491	0.025		0.196	0.251	0.172	0.093			0.240	0.015	0.199	0.111		0.048	0.077			0.092	0.037		0.081	0.327	0.064	0.657
Excess CaO + MgO																									0.106
Excess Na_2O							0.317	0.225	0.300					0.046	0.269		0.024	0.108	0.245		0.016			0.186	0.483
Excess B_2O_3																				0.110					0.289
Excess Li_2O		0.091																							0.359

APPENDIX I

The React module of The Geochemist's Workbench® release 4.0.3 (GWB) was used to predict mineral precipitates from Product Consistency Test (PCT) leachates. Elemental analyses of leachates in ppm were converted to mmol/l and input into GWB. Mineral precipitates were then extracted from the GWB output. A sample React input file is shown in Table 5.

Table 5. Sample React Script

React Command	Explanation
T = 90	PCT temperature in °C
swap $O_2(g)$ for $O_2(aq)$	Swaps oxygen gas into the system.
f $O_2(g)$ = 0.2	Sets the oxygen fugacity to that of air. It is assumed that the gas in the PCT leach vessel is atmospheric.
print species long dxprint = 1	Controls the output file content and length.
suppress Quartz Amrph^silica Cristobalite Hematite Epidote Epidote-ord suppress Andradite Borax Tridymite Chalcedony Prehnite	These minerals are prevented from precipitating.
swap $Al(OH)^{4-}$ for Al^{+++} swap $Fe(OH)^{4-}$ for Fe^{++} swap OH- for H^+	While the program will properly speciate cations such as Al^{3+} and Fe^{2+}, there are less iterations if the cation is swapped for a more likely species.
$SiO_2(aq)$ = 1.878 mmolar Na^+ = 2.31 mmolar $B(OH)_3$ = 4.488 mmolar $Al(OH)^{4-}$ = 0.65 mmolar Ca^{++} = 0.00168 mmolar $Fe(OH)^{4-}$ = 0.00644 mmolar OH^- = 0.001 molal balance on OH^-	This is the solution composition in milimoles per liter. For OH-, this is only an initial values. the balance command allows the software to adjust OH- concentration to obtain the charge balance.

11.0 REFERENCES

1 A.C. Lasaga and A. Luttge, **"Mineralogical Approaches to Fundamental Crystal Dissolution Kinetics,"** Am. Mineralogist, 89, 527-540 (2004).

2 P. Aagaard and H. C. Helgeson, **"Thermodynamic and Kinetic Constraints on Reaction Rates Among Minerals and Aqueous Solutions, I. Theoretical Considerations,"** Amer. J. Sci., 282, 237-285 (1982).

3 A.C. Lasaga, "**Chemical Kinetics of Water-Rock Interactions,"** J. Geophys. Res., B6, 4009-40025 (1984).

4 W. Ebert, **"Defense High Level Waste Glass Degradation,"** Office of Civilian Radioactive Waste Management Analysis/Model, ANL-EBS-MD-000016, Rev.00 ICN01(December, 2000).

5 H.C. Helgeson, W.M. Murphy, and P. Aagaard, **"Thermodynamic and Kinetic Constraints on Reaction Rates Among Minerals and Aqueous Solutions, II. Rate Constants, Effective Surface Area, and the Hydrolysis of Feldspar,"** Geochimica et Cosmochimica Acta, 48, 2405-2432 (1984).

6 E.H. Oelkers, **"General Kinetic Description of Multioxide Silicate Mineral and Glass Dissolution,"** Geochim. Cosmochim. Acta, 65 [21], 3703-3719 (2001).

7 E.H. Oelkers, J. Schott and J.L. Devidal, **"The effect of Aluminum, pH and Chemical Affinity on the Rates of Aluminosilicate Dissolution Reactions,"** Geochim. Cosmochim. Acta, 58, 2011-2024 (1994).

8 E. Wieland, B. Wehrli, and W. Stumm, **"The Coordination Chemistry of Weathering: III. A generalization on the Dissolution Rates of Minerals,"** Geochim. Cosmochim. Acta, 52[8], 1969-1981 (1988).

9 A.C. Lasaga, **"Fundamental Approaches in Describing Mineral Dissolution and Precipitation Rates,"** Reviews in Mineralogy, V.31, 23-86 (1995).

10 E.H. Oelkers and S.R. Sislason**, "The Mechanism, Rates, and Consequences of Basaltic Glass Dissolution: I. An Experimental Study of the Dissolution Rates of basaltic Glass as a Function of Aqueous Al, Si, and Oxalic Acid Concentration at 25°C and pH = 3 and 11,"** Geochim. Cosmochim. Acta, 65 [21], 3671-3681 (2001).

11 Y. Linard, T. Advocat, C. Jegou, P. Richet**, "Thermochemistry of Nuclear Waste Glasses: Application to Weathering Studies,"** J. Non-Crystalline Solids 289, 135-143 (2001).

12 S. Gin, **"Control of R7T7 Nuclear Glass Alteration Kinetics under Saturation Conditions,"** Sci. Basis for Nuclear Waste Management XIX, W.M. Murphy and D.A. Knecht (Eds.), Materials Research Society, Pittsburgh, PA, 189-196 (1996).

13 E. Vernaz, S. Gin, C. Jegou, and I. Ribet, **"Present Understanding of R7T7 Glass Alteration Kinetics and Their Impact on Long-Term Behavior Modeling"** J. Nucl. Materials, 298 (1-2), 27-36 (2001).

14 M. Lagache, **"New Data on the Kinetics of the Dissolution of Alkali Feldspars at 200°C in CO_2 Charged Water,"** Geochim.Cosmochim. Acta, 40, 157-161 (1976).

15 J.P. Hamilton, S.L. Brantley, C.G. Pantano, L.J. Criscenti, and J.D. Kubicki, **"Dissolution of Nepheline, Jadeite, and Albite Glasses: Toward Better Models for Aluminosilicate Dissolution,"** Geochemica et Cosmochimica Acta, 65 [21], 3683-3702 (2001).

16 N. Tsomaia, **"Solid-State Nuclear Magnetic Resonance Investigations of Surface Layers in Oxide Glass Systems,"** Unpublished Ph.D. Thesis, The Pennsylvania State University, (May 2002).

17 N Tsomaia, S.L. Brantley, J.P. Hamilton, C.G. Pantano, and K.T. Mueller, **"Solid State NMR Studies of Aluminate and Silicate Environments in Surface Layers of Leached Aluminosilicate Glasses and Crystals: Implications for Dissolution,"** American Mineralogist, 88, 54-67 (2003).

18 R. Hellmann, C.M. Eggleston, M.F. Hochella, Jr. and D.A. Crerar**, "The Formation of Leached Layers on Albite Surfaces During Dissolution Under Hydrothermal Conditions,"** Geochim. Cosmochim. Acta, 54, 1267-1281 (1990).

19 R. Hellmann, C.M. Eggleston, M.F. Hochella, Jr. and D.A. Crerar**, "The Formation of Leached Layers on Albite Surfaces During Dissolution Under Hydrothermal Conditions,"** Geochim. Cosmochim. Acta, 54, 1267-1281 (1990).

20 P. Van Iseghem and B. Grambow, **"The Long-Term Corrosion and Modeling of Two Simulated Belgian Reference High-Level Waste Glasses,"** Sci. Basis for Nuclear Waste Management XI, J.J. Apted and R.E. Westerman (Eds.), Materials Research Society, Pittsburgh, PA, 631-639 (1987).

21 Y. Inagaki, K. Idemitsu, T. Arima, T. Maeda, H. Ogawa, F. Itonaga**, "Alteration-Phase Formation and Associated Cesium Release During Alteration of R7T7 Waste Glass,"** Scientific Basis for Nuclear Waste Mgt. XXV, B.P. McGrail and G.A. Cragnoliono (Eds.), Materials Research Society, Pittsburgh, PA., 589-596 (2002).

22 T.A. Abrajano, J.K. Bates, and C.D. Byers, **"Aqueous Corrosion of Natural Nuclear Waste Glasses. I. Comparative Rates of Hydration in Liquid and Vapor Environments at Elevated Temperatures,"** J. Non-Cryst. Solids 84, 251-257 (1986).

23 D.M. Strachan and T.L. Croak, **"Compositional Effects on Long-Term Dissolution of Borosilicate Glass,"** J. Non-Crystalline Solids, 272, 22-33 (2000).

24 American Society for Testing and Materials, **"Standard Practice for Prediction of the Long-Term Behavior of Waste Package Materials Including Waste Forms Used in the Geologic Disposal of High-Level Nuclear Waste,"** ASTM Standard C1174.

25 J.E. Mendel (Compiler), **Final Report of the Defense High-Level Waste Leaching**

Mechanisms Program, US DOE Report PNL-5157, Battelle Pacific Northwest Laboratories, Richland WA (1984).

26 L.L.Hench and D.E. Clark, "**Surface Properties and Performance Prediction of Alternative Waste Forms,"** NUREG/CR-3472, Vol. 2 (1986).

27 R.W. Douglas and T.M.M. El-Shamy, **"Reactions of Glasses with Aqueous Solutions,"** J. Am. Ceram. Soc., 50[1], 1-8 (1967)

28 C.M. Jantzen, **"Thermodynamic Approach to Glass Corrosion,"** Corrosion of Glass, Ceramics, and Ceramic Superconductors, D.E. Clark and B.K. Zoitos, Noyes Publications, Park Ridge, NJ, 153-215 (1992).

29 R.M. Wallace and G.G. Wicks, **"Leaching Chemistry of Defense Borosilicate Glass,"** *Scientific Basis for Nuclear Waste Management, VI*, D.G. Brookins (Ed.), Elsevier North Holland, New York, 23-28 (1983).

30 G.G. Wicks, W.C. Mosley, P.G. Whitkop, and K.A. Saturday, **"Durability of Simulated Waste Glass-Effects of Pressure and Formation of Surface Layers,"** J. Non-Cryst. Solids, 49, 413-28 (1982).

31 C.M. Jantzen, D.R. Clarke, P.E.D. Morgan, and A.B. Harker, "**Leaching of Polyphase Nuclear Waste Ceramics: Microstructural and Phase Characterization,"** J. Am. Ceram. Soc., 65[6]. 292-300 (1982).

32 A. Gauthier, P. LeCoustumer, and J-H. Thomassin, **"Nature and Effect of the Alteration Layer During Nuclear Waste Glass Dissolution,"** Scientific Basis for Nuclear Waste Mgt. XXV, B.P. McGrail and G.A. Cragnoliono (Eds.), Materials Research Society, Pittsburgh, PA., 555-561 (2002).

33 L.L. Hench and D.E. Clark, **"Physical Chemistry of Glass Surfaces,"** J. Non-Cryst. Solids, 28, 83-105 (1978).

34 A.B. Woodland, J.K. Bates, T.J. Gerding, **"Parametric Effects on Glass Reaction in the Unsaturated Test Method,"** U.S. DOE Report ANL-91/36, Argonne National Laboratory, Argonne, IL, 130pp (December, 1991).

35 J.K. Bates, C.R. Bradley, E.C. Buck, J.C. Cunnane, N.L. Dietz, W.L. Ebert, J.W. Emery, R.C. Ewing, X. Feng, T.J. Gerding, M. Gong, W.-T Han, J.C. Hoh, J.J. Mazer, M. Tomozawa, L.-M. Wang, and D.J. Wronkiewicz, **"ANL Technical Support Program for DOE Environmental Restoration and Waste Management, Annual Report October 1990-September 1991**," US DOE Report ANL-92/9, Argonne National Laboratory, Argonne, IL, 149pp (March, 1992).

36 X. Feng, J.C. Cunnane, and J.K. Bates, **"A Literature Review of Surface Alteration Layer Effects on Waste Glass Behavior,"** Ceramic Transactions, V. 39 , G.B. Mellinger (Ed.), American Ceramic Society, Westerville, OH, 341-352 (1994).

37 A.K. Bandyopadhyai, R. Jabra, and J. Phalippou, **"Association of OH Groups with Boron and Silicon Atoms in SiO_2-B_2O_3 Glasses by Infrared Spectroscopy,"** J. Mat. Sci. Letters,

8[12], 1464-1467 (1989).

38 R.J. Charles, **"Static Fatigue of Glass, I and II,"** J. of Applied Physics, 29 [11] 1549-1560 (1958).

39 J.K. Bates and L.J. Jardine, **"Hydration Aging of Nuclear Waste Glass,"** Science, 218, 51-52 (1982).

40 F. C. Perez-Cardenas, Hao Gan, Xiaodong Lu, and I.L. Pegg, **"Mechanism of Vapor Phase Hydration in High Sodium Waste Glasses from Computer Simulations,"** Scientific Basis for Nuclear Waste Mgt. XXV, B.P. McGrail and G.A. Cragnoliono (Eds.), Materials Research Society, Pittsburgh, PA., 581-588 (2002).

41 W.L. Ebert, **"The Effects of the Glass Surface Area/Solution Volume Ratio on Glass Corrosion: A Critical Review,"** U.S. DOE Report ANL-94/34, Argonne National Laboratory, Argonne, IL, 289p (March 1995).

42 W.L. Ebert, E.C. Buck, J.S. Luo, S.W. Tam, and J.K. Bates, **"Corrosion Behavior of Environmental Assessment Glass in Product Consistency Tests of Extended Duration,"** U.S. DOE Report ANL-98/27, Argonne National Laboratory, Argonne, IL, 69p (September 1998).

43 C.M. Jantzen, **"Prediction of Glass Durability as a Function of Environmental Conditions,"** Proceedings of the Symposium on Materials Stability and Environmental Degradation, A. Barkatt et al. (Eds.), Materials Research Society, Pittsburgh, PA, 143-159 (1988).

44 C.M. Jantzen, **"Prediction of Glass Durability as a Function of Glass Composition and Test Conditions: Thermodynamics and Kinetics,"** Proceedings of the First Intl. Conference on Advances in the Fusion of Glass, American Ceramic Society, Westerville, OH, p.24.1-24.17 (1988).

45 J.K. Bates, E.C. Buck, N.L. Dietz, T. DiSanto, W.L. Ebert, J.W. Emery, J.A. Fortner, L.D. Hafenrichter, J.C. Hoh, J.S. Luo, L. Nunez, M.T. Surchik, S.F. Wolf, and D.J. Wronkiewicz, **"ANL Technical Support Program for DOE Office of Environmental Management,"** U.S. DOE Report ANL-96/11, Argonne National Laboratory, Argonne, IL (July, 1996).

46 G.G. Wicks, **"Nuclear Waste Glasses: Corrosion Behavior and Field Tests,"** *Corrosion of Glass, Ceramics, and Ceramic Superconductors*, D.E. Clark and B.K. Zoitos, Noyes Publications, Park Ridge, NJ, 218-268 (1992).

47 G.G. Wicks, P.E. O'Rouke, and P.G. Whitkop, **"The Chemical Durability of Savannah River Plant Waste Glass as a Function of Groundwater pH,"** U.S. DOE Report DP-MS-81-104, E.I. duPont deNemours & Co., Savannah River Laboratory, Aiken, SC (May, 1982).

48 W.L. Ebert, J.K. Bates, C.R. Bradley, E.C. Buck, N.L. Dietz, and N.R. Brown, **"The Long-Term Alteration of Borosilicate Waste Glasses,"** Ceramic Transactions V.39, American Ceramic Society, Westerville, OH, 333-340 (1994).

49 X. Feng, J.C. Cunnane, and J.K. Bates, **"A Literature Review of Surface Alteration Layer Effects on Waste Glass Behavior,"** *Ceramic Transactions, V. 39* , G.B. Mellinger (Ed.), American Ceramic Society, Westerville, OH, 341-352 (1994).

50 A.B. Woodland, J.K. Bates, T.J. Gerding, **"Parametric Effects on Glass Reaction in the Unsaturated Test Method,"** U.S. DOE Report ANL-91/36, Argonne National Laboratory, Argonne, IL, 130pp (December, 1991).

51 J.K. Bates, C.R. Bradley, E.C. Buck, J.C. Cunnane, N.L. Dietz, W.L. Ebert, J.W. Emery, R.C. Ewing, X. Feng, T.J. Gerding, M. Gong, W.-T Han, J.C. Hoh, J.J. Mazer, M. Tomozawa, L.-M. Wang, and D.J. Wronkiewicz," **ANL Technical Support Program for DOE Environmental Restoration and Waste Management, Annual Report October 1990-September 1991,"** US DOE Report ANL-92/9, Argonne National Laboratory, Argonne, IL, 149pp (March, 1992).

52 D.J. Wronkiewicz, J.K. Bates, E.C. Buck, J.C. Hoh, J.W. Emery, and L.M. Wang, **"Radiation Effects in Moist-Air Systems and the Influence of Radiolytic Product Formation on Nuclear Waste Glass Corrosion,"** U.S. DOE Report ANL-97/15, Argonne National Laboratory, Argonne, IL (July, 1997).

53 E.C. Buck, J.A. Fortner, J.K. Bates, X. Feng, N.L. Dietz, C.R. Bradley, and B.S. Tani, **"Analytical Electron Microscopy Examination of Solid Reaction Products in Long-Term Tests of SRL 200 Waste Glasses,"** Scientific Basis for Nuclear Waste Mgt. XVII, A. Barkatt and R.A. VanKonynenburg (Eds), Materials Research Society, Pittsburgh, PA, 585-593 (1994).

54 J.S. Luo, T.A. Abrajano, Jr., and W.L. Ebert, **"Natural Analogues of Nuclear Waste Glass Corrosion,"** U.S. DOE Report ANL-98/22, Argonne National Laboratory, Argonne, IL (September, 1998).

55 L.L. Ames and L.B. Sand**, "Factors Effecting Maximum Hydrothermal Stability in Montmorillonites,"** *Am. Mineralogist, 43,* 461-468 (1958).

56 R.Roy and L.B. Sand, **"A Note on Some Properties of Synthetic Montmorillonites,"** *Am. Mineralogist, 41*, 505-509 (1956).

57 R. Roy and E.F. Osborn, **"The System Al_2O_3-SiO_2-H_2O,"** *Am. Mineralogist, 39*, 853-885 (1954).

58 R.A. Sheppard, **"Zeolitic Diagenesis of Tuffs in the Miocene Chalk Hills Formation, Western Snake River Plain, Idaho,"** U.S. Geological Survey Bulletin, 27p (1963).

59 B.H.W. S. deJong, C.M. Schramm, and V.E. Parziale, **"Polymerization of Silicate and Aluminate Tetrahedra in Glasses, Melts, and Aqueous Solutions, IV. Aluminum Coordination in Glasses and Aqueous Solutions and Comments on the Aluminum Avoidance Principle,"** *Geochim. Cosmochim. Acta, 47*, 1223-1236 (1983).

60 A.F. White, **"Weathering Characteristics of Natural Glass and Influences on Associated Water Chemistry,"** *J. Non-Cryst. Solids, 67*, 225-244 (1984)

61 R.A. Sheppard and A.J. Gude, **"Distribution and Genesis of Authigenic Silicate Minerals in Tuffs of Pleistocene Lake Tecopa, Inyo County, California, "** US Geol. Survey Prof. Paper 597, 38p. (1968)

62 D. Savage and N.A. Chapman, **"Hydrothermal Behavior of Simulated Waste Glass- and Waste-Rock Interactions under Repository Conditions,"** *Chem. Geol., 36*, 59-86 (1982).

63 J.K. Bates, C.R. Bradley, N.L. Dietz, W.L. Ebert, J.W. Emery, T.J. Gerding, J.C. Hoh, J.J. Mazer, and J.E. Young, **"Unsaturated Glass Testing for DOE Program in Environmental Restoration and Waste Management, Annual Report, October 1989-September 1990,"** U.S. DOE Report ANL-90/40, Argonne National Laboratory, Argonne, IL (1991).

64 M.E. Morgenstein and D.L. Shettel, Jr., **"Evaluation of Borosilicate Glass as a High-Level Radioactive Waste Form,"** High Level Radioactive Waste Management, Proc. Fourth Annual International Conf., Vol. 2, Am. Nuclear Soc, La Grange Park, IL, 1728-1734 (1993)

65 R.C. Ewing, **"Natural Glasses: Analogues for Radioactive Waste Forms,"** Scientific Basis for Nuclear Waste Management, I, G.J. McCarthy (Ed)., Plenum Press, New York, 57-68 (1979).

66 G. Malow, W. Lutze and R.C. Ewing, **"Alteration Effects and Leach Rates of Basaltic Glasses: Implications for the Long-Term Stability of Nuclear Waste Form Borosilicate Glasses,"** J. Non-Cryst. Solids, 67, 305-321 (1984).

67 C.C. Allen, **"Stability and Alteration of Naturally Occurring Low-Silica Glasses: Implications for the Long Term Stability of Waste Form Glasses,"** Sci. Basis for Nuclear Waste Mgt. V, W. Lutze (Ed.), Elsevier Science Publ., New York, 37-44 (1982).

68 C.M. Jantzen and M.J. Plodinec, **"Thermodynamic Model of Natural, Medieval, and Nuclear Waste Glass Durability,"** J. Non-Crystalline Solids, 67, 207-233 (1984).

69 W.L. Bourcier, D.W. Peiffer, K.G. Knauss, K.D. McKeegan, and D.K. Smith, **"Model for Borosilicate Glass Dissolution Based on Dissolution Affinity of a Surface Alteration Layer,"** Scientific Basis for Nuclear Waste Management, XIII, V.M. Oversby and P.W. Brown (Eds.) Materials Research Society, Pittsburgh, PA, Volume 176, 209-216 (1990).

70 W.L. Ebert and J.K. Bates, **"The Reaction of Synthetic Nuclear Waste Glass in Steam and Hydrothermal Solution,"** Scientific Basis for Nuclear Waste Mgt. XIII, V.M. Oversby and P.W. Brown (Eds.), Materials Research Society, Pittsburgh, PA, 339-346 (1990).

71 P.C. Burns, R.A. Olson, R.J. Finch, J.M. Hanchar, and Y. Thibault, **"$KNa_3(UO_2)_2(Si_4O_{10})_2(H_2O)_4$, a New Compound Formed During Vapor Hydration of an Actinide-Bearing Borosilicate Waste Glass,"** J. Nuclear Materials, 278, 290-300 (2000).

72 W.G. Ramsey, **"Glass Dissolution Chemistry of the System Na_2O-B_2O_3-SiO_2-Al_2O_3-Fe_2O_3-CaO,"** Unpublished Ph.D. Thesis Clemson University, 202pp (1995).

73 C.A. Cicero, **"Final Report: Product Consistency Test Algorithm for DWPF Product Control,"** U.S. DOE Report WSRC-TR-95-00453, Rev. 0, Westinghouse Savannah River Co., Savannah River Technology Center, Aiken, SC (April 19, 1995).

74 A.L. Kielpinski WSRC-NB-94-319.

75 J.M. Pareizs, **"Purex Sludge Durability Crucible Studies,"** U.S. DOE Report WSRC-TR-95-0154, Rev. 0, Westinghouse Savannah River Co., Savannah River Technology Center, Aiken, SC (May 5, 1995).

76 M.K. Andrews WSRC-NB-92-151.

77 D.K. Peeler and T.B. Edwards**, "Impact of REDOX on Glass Durability: Experimental Results,"** U.S. DOE Report WSRC-TR-2004-00313, Rev. 0, Savannah River National Laboratory, Aiken, SC (June 2004) and WSRC-NB-2003-00047.

78 C.M. Jantzen, K.G. Brown, T.B. Edwards, and J.B. Pickett, U.S. Patent #5,846,278, **"Method of Determining Glass Durability (THERMO™)"** (December 8, 1998)

79 C.M. Jantzen, J.B. Pickett, K.G. Brown, T.B. Edwards, and D.C. Beam, **"Process/Product Models for the Defense Waste Processing Facility (DWPF): Part I. Predicting Glass Durability from Composition Using a Thermodynamic Hydration Energy Reaction MOdel (THERMO),"** U.S. DOE Report WSRC-TR-93-0672, Westinghouse Savannah River Co., Savannah River Technology Center, Aiken, SC, 464p. (September, 1995).

80 S.L. Marra, and C.M. Jantzen, **"Characterization of Projected DWPF Glasses Heat Treated to Simulate Canister Centerline Cooling,"** U.S. DOE Report WSRC-TR-92-142, Westinghouse Savannah River Co., Savannah River Technology Center, Aiken, SC, 38p (May, 1992).

81 C.M. Jantzen, N.E. Bibler, D.C. Beam, C.L. Crawford, C.L., S.L. Marra, A.A. Ramsey, and M.A. Pickett, **"Development and Characterization of the Defense Waste Processing Facility (DWPF) Waste Compliance Plan (WCP) Glasses,"** US DOE Report WSRC-TR-93-181, Westinghouse Savannah River Co., Savannah River Technology Center, Aiken, SC (in preparation).

82 C.M. Jantzen, N.E. Bibler, D.C. Beam, and M.A. Pickett, **"Characterization of the**

Defense Waste Processing Facility (DWPF) Environmental Assessment (EA) Glass Standard Reference Material," U.S. DOE Report WSRC-TR-92-346, Rev.1, Westinghouse Savannah River Co., Savannah River Technology Center, Aiken, SC, 92p (February, 1993).

83 C.M. Jantzen, N.E. Bibler, D.C. Beam, D.C. and M.A. Pickett, "**Development and Characterization of the Defense Waste Processing Facility (DWPF) Environmental Assessment (EA) Glass Standard Reference Material,"** Environmental and Waste Management Issues in the Ceramic Industry, Ceramic Transactions, 39, American Ceramic Society, Westerville, OH, 313-322 (1994).

84 C.M. Jantzen, K.G. Brown, J.B. Pickett, and G.L. Ritzhaupt, **"Crystalline Phase Separation in Phosphate Containing Waste Glasses: Relevance to INEEL HAW,"** U.S. DOE Report WSRC-TR-2000-00339, Westinghouse Savannah River Co., Savannah River Technology Center, Aiken, SC (September 30, 2000).

85 I. Tovena, T. Advocat, D. Ghaleb, E. Vernaz and F. Larche, **"Thermodynamic and Structural Models Compared with the Initial Dissolution Rates of SON Glass Samples,"** Sci. Basis for Nucl. Waste Mgt., XVII, A. Barkatt and R.A. Van Konynenburg (Eds.), Mat. Res. Soc., Pittsburgh, PA, 595-602 (1994).

86 C.M. Jantzen, and K.G. Brown, **"Impact of Phase Separation on Waste Glass Durability,"** Environmental Issues and Waste Management Technologies in the Ceramic and Nuclear Industries, V, G. T. Chandler (Eds.), Ceramic Transactions, V. 107, 289-300 (2000).

87 T.J. Wolery, **"Calculation of Chemical Equilibrium between Aqueous Solution and Minerals: The EQ3/6 Software Package,"** UCRL-52658, Lawrence Livermore Laboratory, Livermore, CA (1979).

88 W.B. White, **"Glass Structure and Glass Durability,"** Materials Stability and Environmental Degradation, A. Barkatt, E.D. Vernik, and L.R. Smith (Eds.), MRS Symposium Proceedings V. 125 (1988).

89 W.T. Huang, **"Petrology,"** McGraw-Hill Book Company, New York, 480pp (1962).

90 R. Conradt, **"A Proposition for an Improved Theoretical Treatment of the Corrosion of Multi-Component Glasses,"** *J. Nucl. Mat. 298,* 19-26 (2001).

91 R. Condrat, **"A Thermodynamic Approach to Multicomponent Oxide Glasses,"** Glastech. Ber. Glass Sci. Technol, 68C1, 43-50 (1995).

92 R. Condrat and P. Pimkhaokham, **"An easy-to-apply Method to Estimate the Heat Demand for Melting Technical Silicate Glasses,"** Glastechn. Ber. 63K, 134-143 (1990).

93 D.J. Stein and F.J. Spera, **"Molecular Dynamics Simulations of Liquids and Glasses in the System $NaAlSiO_4$-SiO_2: Methodology and Melt Structures,"** *Am. Mineralogist, 80,* 417-431 (1995).

94 B.M.J. Smets & T.P.A. Lommen, **"The Incorporation of Aluminum Oxide and Boron Oxide in Sodium Silicate Glasses, Studied by X-Ray Photoelectron Spectroscopy,"** *Phys. Chem. Glasses, 22* [*6*], 158-162 (1981).

95 K.L. Geisinger, R. Oestrike, Al Navrotsky, G.L. Turner, and R.J. Kirkpatrick, **"Thermochemistry and Structure of Glasses Along the Join $NaAlSi_3O_8$-$NaBSi_3O_8$,"** *Geochim. Cosmochim Acta, 52*, 2405-2414 (1988).

`

96 W.C. LaCourse and A.N. Cormack, **"Glasses with Transitional Structures,"** Advances in the Fusion and Processing of Glass, II, A.G. Clare and L.E. Jones (Eds.), Ceramic Transactions V. 82, 273-279 (1998).

97 Y. Cao and A.N. Cormack, **"A Structural Model for Interpretation of an Anomaly in Alkali Aluminosilicate Glasses at Al/Alkali= 0.2-0.4,"** Diffusion in Amorphous Materials, H. Jain and D. Gupta (Eds.), The Materials Society Warrendale, PA, 137-152 (1994).

98 M.E. Fleet, **"Tetrahedral-site Occupancies in Reedmergnerite and Synthetic Boron Albite ($NaBSi_3O_8$),"** *Am. Mineralogist, 77*, 76-84 (1992).

99 W.G. Ramsey, C.M. Jantzen, and T.D. Taylor, **"Relationship Between Borosilicate Glass Composition, Structure, and Durability Test Response,"** Ceramic Transactions, V.29, American Ceramic Society, Westerville, OH, 325-332 (1994).

100 B.P. McGrail, J.P. Icenhower, and E.A. Rodriguez, **"Origins of Discrepancies Between Kinetic Rate Law Theory and Experiments in the Na_2O-B_2O_3-SiO_2 System,"** Scientific Basis for Nuclear Waste Management, XXV, Materials Research Society, Pittsburgh, PA, 537-546 (2002).

101 J.G. Darab, X. Feng, J.C. Linehan, P.A. Smith, and I. Roth, **"Composition-Structure Relationships in Model Hanford Low-Level Waste Glasses,"** Ceramic Transactions, V. 72, American Ceramic Society, Westerville, OH, 103-110 (1996).

102 B.M.J. Smets and D.M. Krol, **"Group III Ions in Sodium Silicate Glass. Part 1. X-ray Photoelectron Spectroscopy Study,"** *Phys. Chem. Glasses, 25 [5],* 113-118 (1984).

103 W.L. Konijnendijk, **"Structural Differences Between Borosilicate and Aluminosilicate Glasses Studied by Raman Scattering,"** *Glastechn. Ber. 48 [10]*, 216-218 (1975).

104 T. Furukawa and W.B. White, **"Raman Spectroscopic Investigation of Sodium Borosilicate Glass Structure,"** *J. Mat. Sci., 16*, 2689-2700 (1981).

105 C.A. Cicero, S.L. Marra, and M.K. Andrews, **"Phase Stability Determinations of DWPF Waste Glasses,"** U.S. DOE Report WSRC-TR-93-227, Rev. 0, Westinghouse Savannah River Co., Aiken, SC (May, 1993).

106 M.K. Andrews, C.A. Cicero, S.L. Marra, D.C. Beam, and C.M. Jantzen, **"Phase Stability Determinations of DWPF Waste Glasses,"** Nucleation and Crystallization in Liquids and Glasses, Ceramic Transactions, v.30, 371-374 (1993).

107 P.R. Hrma and G.F. Piepel, **"Property/Composition Relationships for Hanford High-Level Waste Glasses Melting at 1150°C, Volume 1"** U.S. DOE Report PNL-10359. Battelle Pacific Northwest Laboratory, Richland, WA (December, 1994).

108 P.R. Hrma and G.F. Piepel, **"Property/Composition Relationships for Hanford High-Level Waste Glasses Melting at 1150°C, Volume 2,"** U.S. DOE Report PNL-10359. Battelle Pacific Northwest Laboratory, Richland, WA (December, 1994).

109 P. Saha, "**Geochemical and X-Ray Investigation of Natural and Synthetic Analcites,"** Am. Mineralogist, 44, 300-313 (1959).